3D CBCT ANALYSIS OF THE FRONTAL SINUS AND ITS RELATIONSHIP TO FORENSIC IDENTIFICATION

Bianaca S. Krus

Submitted to the faculty of the University Graduate School
in partial fulfillment of requirements
for the degree
Master of Arts
in the Department of Anthropology,
Indiana University

July 2014

Accepted by the Graduate Faculty, Indiana University, in partial fulfillment of the requirements for the degree of Master of Arts.

Master's Thesis Committee

_____
Jeremy J. Wilson, Ph.D., Chair

_____
John M. Starbuck, Ph.D.

_____
Richard E. Ward, Ph.D.

ACKNOWLEDGEMENTS

I would first like to thank my husband, Tony, for his constant support and encouragement; my family for always believing in me; Jeremy Wilson, John Starbuck, and Richard Ward for their guidance in completing this project; the Imaging Center within the Indiana University School of Dentistry for financial support; and anyone else who has provided me with works of encouragement throughout this process.

Bianaca S. Krus

3D CBCT ANALYSIS OF THE FRONTAL SINUS AND ITS RELATIONSHIP TO FORENSIC IDENTIFICATION

The positive identification of human remains that are decomposed, burnt, or otherwise disfigured can prove especially challenging in forensic anthropology, resulting in the need for specialized methods of analysis. Due to the unique morphological characteristics of the frontal sinus, a positive identification can be made in cases of unknown human remains, even when remains are highly cremated or decomposed. This study retrospectively reviews 3D CBCT images of a total of 43 Caucasian patients between the ages of 20-38 from the Indiana University School of Dentistry to quantify frontal sinus differences between adult males and females and investigate the usefulness of frontal sinus morphology for forensic identification. Digit codes with six sections and eleven-digit numbers were created to classify each individual sinus. It was shown that 3D CBCT images of the frontal sinus could be used to make a positive forensic identification. Metric measurements displayed a high degree of variability between sinuses and no two digit codes were identical. However, it was also shown that there were almost no quantifiable and significant sexually dimorphic differences between male and female frontal sinuses. This study confirms that sex determination should not be a primary goal of frontal sinus analysis and highlights the importance of creating a standard method of frontal sinus evaluation based on metric measurements.

Jeremy J. Wilson, Ph.D., Chair

TABLE OF CONTENTS

LIST OF TABLES

LIST OF FIGURES

Chapter One – Introduction

The positive identification of unknown persons is an important issue in forensic anthropology and allied sciences involved in medico-legal investigations. The identification of human remains that are decomposed, burnt, or otherwise disfigured can prove especially challenging, resulting in the need for specialized methods of analysis (Belaldavar et al. 2014; Cox et al. 2009; Jablonski and Shum 1989). Methods of analysis such as DNA testing, fingerprints, dental records, and the comparison of antemortem and postmortem radiographs have played important roles in the field of forensic science (Steadman et al., 2006). Several investigators have used conventional radiographs to measure the paranasal sinuses and assess differences among populations (Kim et al. 2013; Tatlisumak et al. 2011). However, recent technological advances in imaging now allow investigators to non-invasively collect ecto- and endo-cranial observations and measurements from three-dimensional (3D) cone-beam computed tomography (CBCT) images. To date, relatively few investigations have been carried out utilizing 3D imaging to assess frontal sinus morphology and its usefulness in forensic identification (Belaldavar et al. 2014; Fourie et al. 2011; Tatlisumak et al. 2011). The morphology of the frontal sinus has been shown to be unique in each individual, even among monozygotic twins (Jablonski and Shum 1989). Due to the unique morphological characteristics of the frontal sinus, a positive identification can be made in cases of unknown human remains, even when they are highly cremated or decomposed (Cox et al. 2009; Steadman et al. 2006). The frontal sinus is also valuable in positive identifications because the structure

changes very little after puberty and is not affected by time elapsed postmortem (Christensen 2004; Jablonski and Shum 1989; Schuller 1943).

This study retrospectively reviews 3D CBCT images of Caucasian patients (n = 43) between the ages of 20-38 yrs. from the Indiana University School of Dentistry to quantify frontal sinus differences between adult males and females and investigate the usefulness of frontal sinus morphology for forensic identification. This study replicates methods used in Kim, et al. (2013) to determine if their proposed method for identification is useful, accurate, and replicable. The presence/absence of the frontal sinus was evaluated, along with the maximal height, width, depth, distance, angle, and volume. Digit codes with six sections and eleven-digit numbers were created to classify each individual sinus. Since the frontal sinus exhibits considerable individual variation, the combined use of metric and non-metric methods could serve as a useful method of analysis for personal identification (Cox et al. 2009; Jablonski and Shum 1989; Steadman et al. 2006). The purpose of this research is to develop a standardized approach to identification based on frontal sinus morphology that will comply with the criteria outlined in the *Daubert v. Merrell Dow Pharmaceuticals, 509 U.S. 579* ruling of 1993.

With the implementation of the *Daubert* criteria, forensic scientists were required to substantiate their assertions with scientifically tested methods and probability assessments (Keierleber and Bohan 2005). This promoted an improvement in quantitative methods for both the testing of hypotheses and probability estimation. The Supreme Court decision in the *Daubert* case

changed approaches to research, evidence, analysis, and expert witness testimony in forensic anthropology (Cameriere et al. 2008; Christensen 2004; Dirkmaat et al. 2008; Keierleber and Bohan 2005; Steadman et al. 2006). Testable, reliable, replicable, and scientifically valid methods are all required for expert testimony under the regulations of the *Daubert* ruling. Along with this, the methods must be tested, have acceptable error rates, be peer-reviewed, have standards that control the technique's operation, and have gained general acceptability within the relevant discipline (Steadman et al. 2006). Dirkmaat and colleagues (2008:35) state that, "testing and replication of the methods and conclusions are an essential part of reliability. Reliability, the ability to produce consistent results, can also be judged by the use of tested scientific acceptance." The validity, or the "measure of how well test results produce correct answers", can then be measured through the use of estimated error rates (Dirkmaat et al. 2008:35-6). With these requirements, the *Daubert* criteria emphasized the importance of the use of replicable methods and standard error rates in forensic anthropology (Cameriere et al. 2008; Christensen 2004; Dirkmaat et al. 2008; Keierleber and Bohan 2005; Steadman et al. 2006).

The following research questions were central to my study and allowed me to evaluate if the proposed method of forensic identification was reliable, replicable, and useful:

- Can a positive forensic identification be made using 3D CBCT images of the frontal sinus?

- Are there quantifiable and significant sexually dimorphic differences between males and females for frontal sinus length, width, depth, and volume?
- Are the methods used by Kim, et al. (2013) easy to replicate?
- Are the methods proposed by Kim, et al. (2013) useful and accurate?
- Is the use of 3D CBCT images an effective use of time in forensic identification?

In Chapter Two, I provide a brief history of the previous research conducted on frontal sinus morphology; this includes the use of the frontal sinus in forensic identifications. In Chapter Three, I present my methods and tools for analyzing the frontal sinus. Chapter Four provides the results of this study, both metric and non-metric. In Chapter Five, I discuss the significance of these results and conclude with suggestions for future research in frontal sinus morphology, including how the proposed methods in this study can be improved upon.

Chapter Two – Review of the Literature

One of the most important aspects of forensic anthropology is the identification of human beings from their skeletal remains (Dirkmaat et al. 2008; Steadman et al. 2006). This process of identification includes the creation of a biological profile consisting of age, sex, ancestry, stature, ante- and perimortem pathologies, and other abnormalities or discriminating features. The need for the identification of an unknown individual is essential in order to complete legal matters, bring relief to loved ones, and justice to victims. The most reliable methods of identification include fingerprints, dental comparisons, and DNA profiling. However, these methods cannot be used when analyzing skeletal remains if DNA is degraded or when there are no DNA samples to use for comparison. The first studies of the frontal sinus revealed important information about its shape, complexity, individuality, and contribution to human identification. In 1921, Schuller (1943) first suggested that the frontal sinus could be used for identification purposes, as was observed by their irregular form in anterior-posterior radiographs. Then in 1925, Culbert and Law used thirteen biometric points found in the frontal sinus to establish the identity of a former patient (Reichs 1993). Since this time, complementary studies have been conducted to examine the anatomical characteristics and variations of the frontal sinus among sexes, different ages, and ethnic groups (Camargo et al. 2007; Nambiar et al. 1999; Reichs 1993).

The frontal sinus is a pneumatic cavity present between the outer and inner tables of the frontal bone, consisting of two air-filled cavities that originate

at the root of the nose and expand superiorly into the peri-glabellar region. The frontal sinus is usually separated by a bony septum and because the left and right sinuses develop independently, it is common that one sinus is larger than the other (Nambiar et al. 1999; Quatrehomme et al. 1996; Tatlisumak et al. 2008). The paranasal sinuses begin development early in fetal life and most anatomical literature suggests that they serve to lighten the skull and add resonance to the voice (Nambiar et al. 1999; Tatlisumak et al. 2011). By the age of six, the frontal sinuses can be seen radiographically and grow larger in size until puberty is completed, usually reaching adult conformation by the age of 20 (Nambiar et al. 1999; Quatrehomme et al. 1996). The frontal sinus is useful in forensic identification due to its irregular shape and individualized characteristics (Camargo et al. 2007; Cox et al. 2009; Nambiar et al. 1999).

It has been shown that the frontal sinus is useful in positive identifications as it is unique in every individual, even monozygotic twins (Jablonski and Shum 1989; Kim et al. 2013). The frontal sinus changes little after the age of 20, although some reports of slight enlargement with age have been noted (Cox et al. 2009; Reichs 1993). The frontal sinus remains unaffected between antemortem and postmortem analysis, maintaining its structure throughout decomposition (Cox et al. 2009; Kim et al. 2013). Sex determination, an important element of forensic investigations of unknown persons, may also be evaluated using the frontal sinus. The accurate prediction of sex of human remains excludes half of the population, thus narrowing down the search for missing persons. Studies using logistic regression analysis of the frontal sinus

have reported that male frontal sinuses are slightly larger than female sinuses, although the differences were not statistically significant (Belaldavar et al. 2014; Camargo et al. 2007; Quatrehomme et al. 1996; Yoshino et al. 1987). The size of the frontal sinus, as measured by surface area, height, width, depth, and volume, has been shown to correlate with body size, height and weight. So while studies have shown the male frontal sinus to be absolutely larger than the female frontal sinus, this is not always the case and may not be worth evaluating as a primary objective (Belaldavar et al. 2014; Camargo et al. 2007; Cox et al. 2009; Reichs 1993), especially when the population of origin is unknown or heterogeneous.

A study by Goyal and colleagues (2012) assessed the frontal sinus for sex determination using univariate and multivariate statistics. However, the univariate Mann-Whitney *U*-tests used to test for sexual dimorphism of the frontal sinus failed to reach statistical significance (p-value ≤ 0.05 considered significant). In addition to this, multivariate logistic regression equations allowed the correct identification of sex in only 60% of cases, which is barely better than chance (i.e. 50%) (Goyal et al. 2012:91). Goyal et al. (2012) and Yoshino et al. (1987) suggested that possible reasons for the low sexual dimorphism may be the frontal sinus' high inter-individual variability, which indicates that the frontal sinus may have limited applications as the sole predictor of sex. Caution must be used when evaluating the frontal sinus for identification purposes, sex determination, or anything else being studied. Environmental factors, diseases, trauma, variations in measurement methodologies and imaging modalities, and

the angle and orientation of the cranium can all modify the image of the frontal sinus and distort identifying characteristics (Camargo et al. 2007; Nambiar et al. 2009; Pfaeffli et al. 2007). Age and ethnicity must also be factored into any analysis, as not all frontal sinus measurements and results are universal (Reichs 1993).

The use of frontal sinus radiographs has become an increasingly accepted technique in forensic identifications and is usually carried out by comparing antemortem and postmortem radiographs. These radiographs are commonly used to make a positive identification of human remains that are decomposed, cremated, or otherwise difficult to identify. Identification by the comparison of radiographs of antemortem and postmortem frontal sinuses is scientifically valid because no two frontal sinuses are alike. However, it has been reported that it is possible for the frontal sinus to be absent altogether in some individuals (7.6% reported by Kim et al. 2013). A large drawback of using radiographs is that data are obtained and observed two-dimensionally, which limits the observers' field of view. Researchers who rely solely on radiographs are restricted to evaluating three-dimensional anatomy in two dimensions, ultimately resulting in a loss of information that could potentially affect research results and conclusions. Because of this limitation and others, three-dimensional computed tomography (CT) and CBCT images are gradually replacing standard two-dimensional radiographs in clinical studies and forensic analyses (Cox et al. 2009; Fourie et al. 2011; Guijarro-Martinez and Swennen 2013).

CT and CBCT three-dimensional images represent an improvement over two-dimensional cephalograms because they allow for increased visualization of the internal structure of the sinus due to the greater detail captured using high-resolution imagery (Guijarro-Martinez and Swennen 2013). CT and CBCT images are acquired using different methods. CT images (formerly referred to as computed axial tomography or "CAT" scans) are created by taking 2D cross-sectional x-rays of an individual or specimen using a single axis of rotation and then using automated visualization software to stack x-ray slices into a single 3D image. The process of creating CBCT images is usually faster and requires a lower radiation dose than traditional CT images. An additional difference is that CBCT images are typically created with subjects in a sitting position, while CT images are often created with subjects in a supine position, which can result in gravitational changes to some structures (Sutthiprapaporn et al. 2008). An analysis by Fourie, et al. (2011) showed that 3D CBCT is both accurate and reliable as a standard method of anthropometric measurement. While it is more common for an individual to have a radiograph or CT in their medical file than a CBCT image, CBCT images are frequently used in the field of dentistry and are more common among dental patients, especially those undergoing orthodontic treatment (Cox et al. 2009; Fourie et al. 2011; Guijarro-Martinez and Swennen 2013).

While the uniqueness of the frontal sinus is widely accepted among the scientific community, most observations are qualitative and subjective, and there is a dearth of quantitative and empirical testing reported in the literature (Cox et

al. 2009:761). In 1987, Yoshino and colleagues proposed a system utilizing several measurements to analyze the frontal sinus such as: surface area bilateral asymmetry of the left and right sinus, superiority of surface area outline of superior borders, partial septa, and supraorbital cells. Using this method, postmortem radiographs were analyzed and the morphological characteristics were given class numbers to form a seven-digit code number. From the arrangement of numbers, frontal sinus patterns could be divided into more than 20,000 possible combinations of code numbers and the chance of two people having identical codes in a small random sample is higher than 1:20,000 (Yoshino et al. 1987). Although there is a greater possibility of two people having identical codes in a large sample, this method could still be useful in creating a positive identification.

The application of Elliptical Fourier Analysis (EFA) to sinuses has been successful in providing quantitative support to the uniqueness of the frontal sinuses (Christensen 2004; Cox et al. 2009). In a 2004 study by Christensen, empirical, quantitative testing was conducted in order to evaluate the uniqueness of frontal sinus outlines. EFA is a geometric morphometric approach that fits a closed curve to an ordered set of data points to outline the frontal sinus and generates a set of coefficients, quantitatively summarizing the outline (Christensen 2004). The results of the study showed that the Euclidean distances between outlines were significantly larger between different individuals than between replicates of the same individual, thus confirming that frontal sinus outlines are unique and individualistic (Christensen 2004). While this technique

is successful, it requires several complex software programs and calculations, which can be time consuming (Christensen 2004; Cox et al. 2009).

Tatlisumak, et al. (2007) used the system FSS: F (presence or absence of frontal sinus), S (intersinus and intrasinus septum), and S (scalloping) to create a simple system for the identification of unknown individuals using CT images of the frontal sinus. It was shown that when adding measurements to this system such as width, height, and length, the results were more accurate than the FSS method alone. Because of this, a combined approach to frontal sinus evaluation of metric and non-metric methods has been thoroughly evaluated and proven to be the most successful in positively identifying individuals (Cox et al. 2009; Tatlisumak et al. 2007; Uthman et al. 2010). A study by Pfaeffli et al. (2007) showed that identification from the frontal sinus is possible using comparisons of images from two different radiological methods, such as antemortem X-rays and postmortem CTs. A study by Cox, et al. (2009) draws upon Christensen's application of EFA and Likelihood Ratios in an effort to simplify this method. Error rates of 0% were achieved using this method; along with demonstrated inter-rater and test-retest reliability (Cox et al. 2009). As a result of these recent studies, methods that have proven to work in the past are quickly becoming outdated and no longer practical. While it has been reported that superimposition of antemortem and postmortem radiographs has allowed for correct identification in 100% of cases, these methods are criticized for being highly subjective and lacking statistical support (Cox et al. 2009; Jablonski and Shum 1989). Coding systems and techniques using classification systems have

been shown to be successful and may offer a solution to this problem (Cox, et al. 2009).

The forensic identification of unknown persons is of vital importance legally, to give justice to victims, and to give closure to friends and family. Any work that can bring us closer to identifying such individuals should be valued and further studied. It has been shown through a review of the literature that there are very few studies that use 3D CBCT images to evaluate frontal sinus measurements. There is also a lack of empirical testing that uses quantitative measurements and statistical applications. Yet, research has shown that the best methods combine metric and non-metric measurements, and utilize some type of coding system that allows for quick and easy analysis of the frontal sinus to assess positive identification (Cox et al. 2009; Kim et al. 2013). Given these recent trends in research, I chose to first replicate a study that uses both metric and non-metric measurements; and then I have taken it two steps further by using CBCT imaging instead of CT imaging, as well as conducting error testing.

Chapter Three – Materials and Methods

A retrospective analysis was performed on 43 CBCT images (0.3mm voxel size; i-Cat machine, Imagine Sciences International LLC, Hatfield, PA) from the IU School of Dentistry. IRB approval was obtained for this study through the IU Human Subjects Office (Study # 1211010075). All identifying patient information was kept confidential, including medical history, and since these images were acquired previously, the data collection efforts did not inconvenience these individuals in any way. This study attempted to replicate methods used in Kim et al. (2013) to determine if their proposed method for forensic identification was useful. Kim et al. (2013) analyzed CT images from 119 Korean cadavers, which were reconstructed in 3D and surveyed using non-metric and metric measurements. Non-metric characteristics included the shape of the frontal sinus in anterior view, the shape of the frontal sinus in lateral view, the outline of the upper border, and the cross-sectional shape (Kim et al. 2013:1). Metric measurements included volume (total, right side, left side, only right, only left), width (fused, right side, left side), distance, height (right side, left side), depth (right side, let side), and angle (anterior, superior) (Kim et al. 2013:7). Measurements were taken from the baseline and digit codes comprising of six sections and a ten-digit number were created in order to identify individuals. CBCT images were analyzed using Dolphin Imaging software (v11.5; Chatsworth, CA) to assess the presence or absence of the frontal sinus and to collect the proposed measurements from each image. Individuals with any illnesses or other identifying markers on the cranium were excluded from the

sample. Only those images with complete frontal sinuses were used. In order to accurately measure sinus volume and surface areas, resolution was standardized by only using CBCT images with a 0.3mm voxel size. To minimize measurement error, an orientation module in Dolphin was used to standardize the orientation of images by passing a horizontal line through orbitale and porion in lateral view and a vertical line through nasion and pogonion in frontal view (Appendix 6.2). As displayed in Table 3.1, a total of 11 Caucasian females and 32 Caucasian males between the ages of 20 and 38 yrs. were evaluated, with a mean age of 23.5 yrs.

Table 3.1: Age Distribution of Males and Females

Age Range (yrs.)	Males	Females
20-24	26	7
25-29	2	4
30-34	3	0
35-39	1	0
Total	32	11

According to Kim et al. the “baseline” was a line drawn horizontally along the upper margin of the orbits and parallel to the Frankfort horizontal plane (2013:5) (Appendix 6.4). In the current study, all non-metric characteristics were evaluated as cut from the baseline. Metric measurements were evaluated as both cut from the baseline, as performed in the study by Kim et al. (2013), and without cutting the frontal sinus from the baseline. When measurements were taken without cutting the frontal sinus from the baseline, the complete frontal

sinus was evaluated and used for measurements. The additional measurements that analyzed the complete frontal sinuses were done in an attempt to improve upon the proposed methods by Kim et al. (2013), which potentially cut off frontal sinus anatomical variation that may be relevant for identification and quantification of human frontal sinus variation.

Non-metric Measurement Methods

Non-metric measurements were collected following methods outlined by Kim et al. (2013). Four non-metric characteristics of the frontal sinus were evaluated and recorded via visual inspection: the shape of the frontal sinus in anterior and lateral views, the outline of the upper border, and the cross-sectional shape of the frontal sinus. The shape of the frontal sinus in anterior view was then classified into eight types: triangle (1), right-angled triangle (2), quadrangle (3), parallelogram (4), trapezoid (5), fan-shaped (6), m-shaped (7), and crown (8) (Table 3.2). The frontal sinus was divided into three types by the shape in lateral view: flat (1), convex (2), and concave (3) (Table 3.3). The outline of the upper border of each side of the frontal sinus was characterized by the number of scallops: flat (0), smooth (1), scallops with two arcades (2), scallops with three arcades (3), scallops with four arcades (4), scallops with five arcades (5), and scallops with six arcades (6) (Table 3.4). The cross-sectional shape of the frontal sinus was classified by the shape of the frontal sinus in inferior view: ellipse (E), crescent (C), square (S), and irregular (I) (Table 3.5).

Table 3.2: Shape of the Frontal Sinus in Anterior View*

Shape of the Frontal Sinus in Anterior View	Digit Code	Illustration
Triangle	1	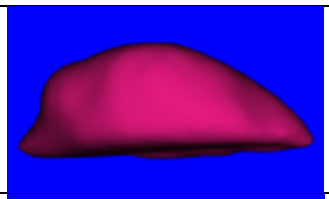
Right-Angled Triangle	2	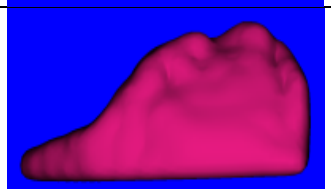
Quadrangle	3	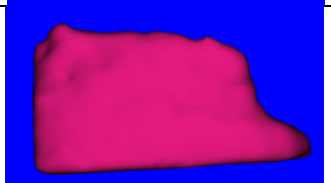
Parallelogram	4	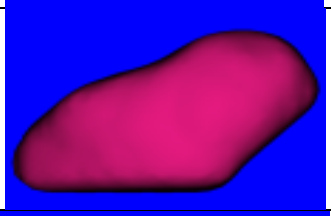
Trapezoid	5	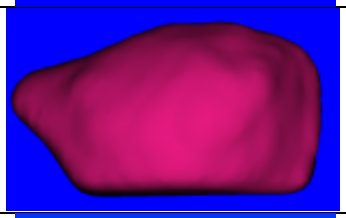
Fan-Shaped	6	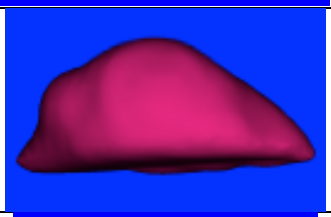
M-Shaped	7	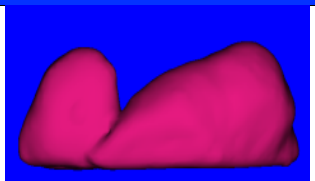
Crown	8	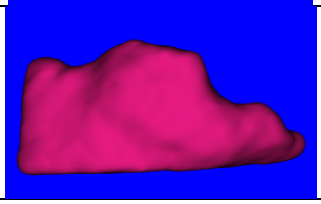

*Frontal Sinus Cut from the Baseline

Table 3.3: Shape of the Frontal Sinus in Lateral View*

Shape of the Frontal Sinus in Lateral View	Digit Code	Illustration
Flat	1	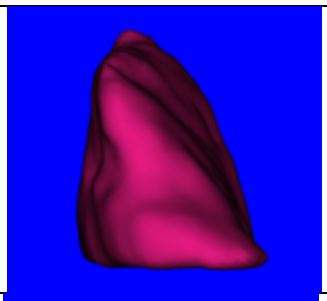
Convex	2	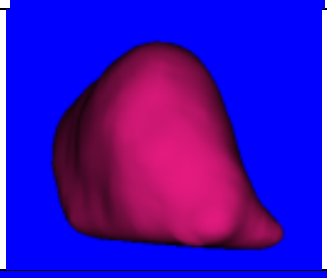
Concave	3	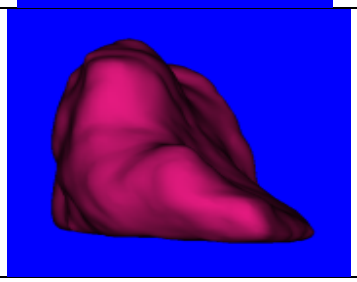

*Frontal Sinus Cut from the Baseline

Table 3.4: Outline of the Upper Border of the Frontal Sinus*

Outline of the Upper Border	Digit Code	Illustration
Flat	0	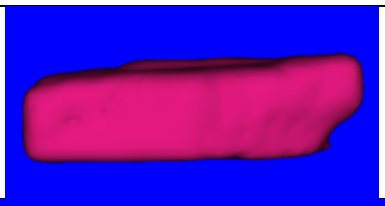
Smooth	1	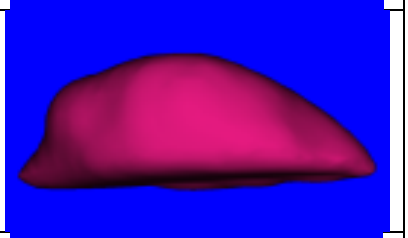
Scallops with two arcades	2	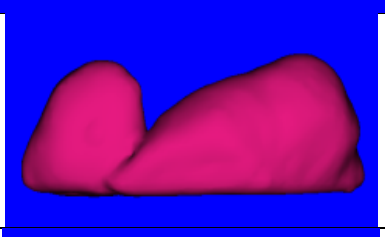
Scallops with three arcades	3	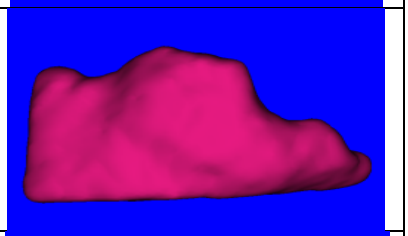
Scallops with four arcades	4	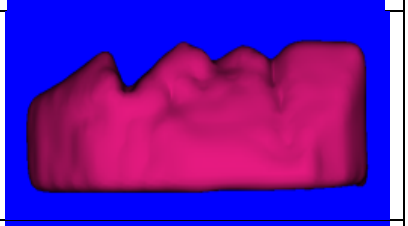
Scallops with five arcades	5	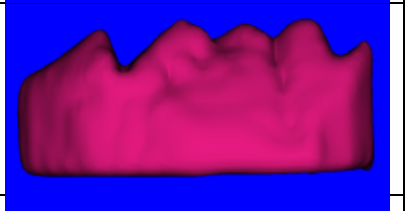
Scallops with six arcades	6	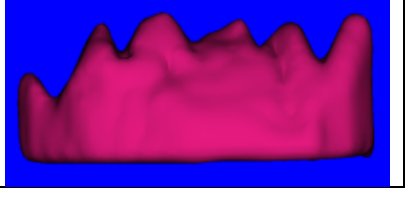

*Frontal Sinus Cut from the Baseline

Table 3.5: Cross-Sectional Shape of the Frontal Sinus*

Cross-Sectional Shape	Digit Code	Illustration
Ellipse	E	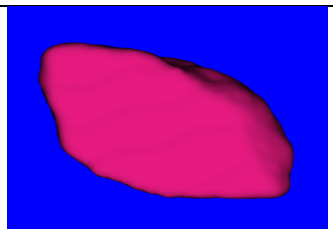
Crescent	C	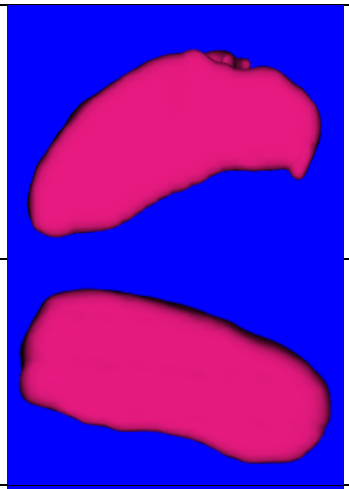
Square	S	
Irregular	I	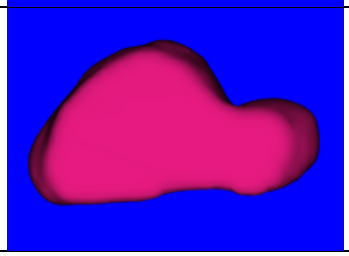

*Frontal Sinus Cut from the Baseline

Metric Measurement Methods

The volume (mm^3), width (mm), distance (mm), height (mm), depth (mm), and angle (º) of each frontal sinus were measured from 3D CBCT images using Dolphin Imaging software (v11.5; Chatsworth, CA) and integrated measurement tools. The results were then analyzed using the statistical program Minitab (v.16) to determine if there were any significant differences. Measurements were first taken when the frontal sinus was cut from the baseline (Table 3.6) following the methods of Kim et al. (2013) and then taken again without cutting the frontal

sinus from the baseline (Table 3.7) to include all frontal sinus anatomy. As the depth and angle were not affected by cutting the frontal sinus from the baseline, these measurements were not re-taken when the complete sinus was evaluated.

Table 3.6: Metric Measurements from the Baseline

Measurements	Definition
Volume* (mm^3)	
Total	Volume of both sinuses
Right Side	Volume of the right frontal sinus
Left Side	Volume of the left frontal sinus
Only Right	Volume of the right frontal sinus when the left is absent
Only Left	Volume of the left frontal sinus when the right is absent
Width* (mm)	
Fused	Maximum width between the most lateral sides of both frontal sinuses if one sinus is fused to the other side
Right Side	Maximum width between the most lateral side and the medial of the right frontal sinus
Left Side	Maximum width between the most lateral side and the medial side of the left frontal sinus
Distance* (mm)	Distance between the highest point of the right frontal sinus and the highest point of the left frontal sinus
Height* (mm)	
Right Side	Maximum height between the baseline and the highest point of the right frontal sinus
Left Side	Maximum height between the baseline and the highest point of the left frontal sinus
Depth (mm)	
Right Side	Depth between the most prominent point of the anterior part and the posterior part of the frontal sinus at the right side
Left Side	Depth between the most prominent point of the anterior part and the posterior part of the frontal sinus at the left side
Angle (º)	
Right Side	Angle between the medial borders of the right and left sinuses
Left Side	Angel between the medial borders of the left and right sinuses

*Measurements taken from the baseline.

Table 3.7: Metric Measurement not from the Baseline

Measurements	Definition
Volume (mm^3)	
Total	Volume of both sinuses
Right Side	Volume of the right frontal sinus
Left Side	Volume of the left frontal sinus
Only Right	Volume of the right frontal sinus when the left is absent
Only Left	Volume of the left frontal sinus when the right is absent
Width (mm)	
Fused	Maximum width between the most lateral sides of both frontal sinuses if one sinus is fused to the other side
Right Side	Maximum width between the most lateral side and the medial of the right frontal sinus
Left Side	Maximum width between the most lateral side and the medial side of the left frontal sinus
Distance (mm)	Distance between the highest point of the right frontal sinus and the highest point of the left frontal sinus
Height (mm)	
Right Side	Maximum height between the lowest point and the highest point of the right frontal sinus
Left Side	Maximum height between the lowest point and the highest point of the left frontal sinus

BAI and Angle

The bilateral asymmetry index (BAI) was calculated using the volume of the right and left frontal sinus by dividing the smaller sinus volume by the larger sinus volume and then multiplying the product by 100. The results were coded as: Bilateral Absence (B), Unilateral Absence (U), $80 \leq BAI$ (1), $60 \leq BAI < 80$ (2), $40 \leq BAI < 60$ (3), $20 \leq BAI < 40$ (4), $BAI < 20$ (5), Fused (F), and Prominent Middle Sinus (M) (Table 3.8). The angle between the left and right sinuses in frontal view were also separately calculated in order to individually identify each sinus. The angle was separated at 10º intervals from 100º. A number from “1” to

"9" was assigned with "1" being below 100º in angle and "9" being over 170º in angle.

Table 3.8: BAI Index

Bilateral Asymmetry Index (BAI)	Digit Code
Bilateral Absence	B
Unilateral Absence	U
80 ≤ BAI (symmetry or almost symmetry)	1
60 ≤ BAI < 80 (slight asymmetry)	2
40 ≤ BAI < 60 (moderate asymmetry)	3
20 ≤ BAI < 40 (strong asymmetry)	4
BAI < 20 (extreme asymmetry)	5
Fused	F
Prominent Middle Sinus	M

Error Study

Because of both instrument imprecision and human inconsistencies, measurements are not free of errors. Technical error of measurement (TEM) is the "variability encountered between dimensions when the same specimens are measured at multiple sessions" (Harris and Smith 2008:S107). A goal of data collection is to minimize the TEM, "which requires repeated measurements [and] enhances the chances of finding a statistically significant difference if one exists" (Harris and Smith 2008:S107). By reducing intra-observer error, which can be assessed and confirmed by calculating TEM, measurement accuracy can be greatly improved (Harris and Smith 2008:S108-9). Increasing measurement

accuracy also has the added effect of increasing the chances of finding a statistically significant difference, if one exists (Harris and Smith 2008:S109). An intra-class correlation (ICC) is a descriptive statistic that can be used to describe how strongly units in the same group resemble each other, and is another method for assessing error (Harris and Smith 2008).

An error study was conducted by measuring ten individuals on two separate occasions with at least 48 hours between each measurement trial in order to avoid memory bias. Trial 1 and Trial 2 were then compared using TEM and ICC. To assess measurement error an ICC was run in SPSS (v.21) for both metric and non-metric measurements. ICC had to be ≥ 0.95 to be considered acceptable. The TEM for metric measurements was calculated in Excel. To be acceptable the TEM value had to be ≤5% of the mean value for a particular trait. In the event that ICC or TEM were considered unacceptable, more trials would have been conducted until the values were acceptable. By conducting these error trials intra-observer error rates were quantified and considered acceptable before collecting data from the entire sample.

Statistical Methods

Both metric and non-metric data were analyzed using Minitab (v.16). To statistically calculate metric measurements *t*-tests and Mann-Whitney tests were performed. Two-sample *t*-tests comparing male and female frontal sinuses were performed. Two-sample t-tests require the assumption of normal distributions to be satisfied in order for the statistics to be valid. However, because the number of females in the sample was small (n = 11), the data were not normally

distributed for each measurement. The nonparametric Mann-Whitney *U* test is a viable alternative to t-tests that does not require data to be distributed normally. Thus, as an exercise in statistical evaluation, both results from two-sample t-tests and nonparametric Mann-Whitney *U* tests are provided with the understanding that the Mann-Whitney results are more statistically robust and exceptionally useful when analyzing small samples. To statistically evaluate non-metric measurements, Chi-Square (χ^2) tests were performed to compare male and female frontal sinuses. The null hypothesis is that the tested variables are independent of sex. A Principal Components Analysis (PCA) was performed on both metric and non-metric data. PCA is a multidimensional ordination analysis that explores patterns of variation in a dataset and does not rely on *a priori* knowledge of a sample's group structure. PCA divides sample variance into principal component axes (PCs) that successively account for the maximum amount of variation in the data while estimating the contribution of each variable to each axis.

Digit Codes

A system of classification of the frontal sinus based on discrete variables was produced. An eleven-digit number represents the four non-metric characteristics and the two metric measurements. Each section of this digit code was described by a two-digit number, except for BAI, and a slash that divides each section. The numbers in each section were divided into right and left frontal sinuses, with the first number representing the right side and the second number representing the left side. The sections were as follows: BAI, the shape in

anterior view, the shape in lateral view, the outline of the upper border, the cross-sectional shape, and the angle between the two sinuses in frontal view. If there was an absence of one sinus it was marked by 'N'. This eleven-digit code was then used to evaluate each of the scans, comparing the uniqueness of each frontal sinus. By assigning a digit code to each individual, with over 20,000 possible combinations, it was possible to assess the uniqueness of each frontal sinus.

Digit Code Comparison Measurements

Once all of the measurements were taken, five individuals from the sample were then measured a second time while blinded to their identity and previous measurements. These measurements were then matched from the blinded individuals to those previously collected from the entire sample, using the digit codes for each. This allowed for the evaluation of the usefulness of actually identifying an individual from the proposed digit code method. This methodology also allowed for a preliminary evaluation of the methods used by Kim et al. (2013) to determine their reliability, effectiveness, and efficiency.

Chapter Four – Results

Frontal sinuses were visible in all 43 of the CBCTs analyzed. There was one incidence of right frontal sinus absence and one incidence of left frontal sinus absence, both in males.

Technical Error of Measurement and Intra-Class Correlation

Technical error of measurement (TEM) and intra-class correlation (ICC) values were both considered acceptable. TEM was assessed for metric values (Table 4.1). If the TEM mean was ≤5% of the mean for each measurement, then the values were considered acceptable. The total volume had a mean of 3389.4mm^3 and a TEM mean of 31.41mm^3. The average right and left volume had a mean of 1721.16mm^3 and a TEM mean of 23.72mm^3. The average right and left width had a mean of 23.26mm and a TEM mean of 0.52mm. The distance had a mean of 34.87mm and a TEM mean of 1.74mm. The average right and left height had a mean of 475.87mm and a TEM mean of 0.42mm. The average right and left depth had a mean of 478.98mm and a TEM mean of 0.30mm. ICC was assessed separately for non-metric values (Table 4.2) and metric values (Table 4.3). The ICC for non-metric measurements was reported at 0.998 for the single measure and 0.999 for the average measure. At the 95% confidence interval for the single measure the lower bound was reported at 0.996 and 0.998 for the upper bound. At the 95% confidence interval for the average measure the lower bound was reported at 0.998 and 0.999 for the upper bound. The ICC for the metric measurements was reported at 1.000 for both the single measure and average measure. At the 95% confidence interval the single

measure for both the lower bound and upper bound were reported at 1.000. At the 95% confidence interval the average measure for both the lower bound and upper bound were reported at 1.000. Both TEM and ICC evaluations showed that non-metric and metric measurements were highly reproducible and accurate.

Table 4.1: Mean Measurement and TEM Values

Measurement	Mean	TEM Mean	TEM ≤ 5%*
Total Volume (mm^3)	3389.4	31.41	YES
Average Right and Left Volume (mm^3)	1721.16	23.72	YES
Average Right and Left Width (mm)	23.26	0.52	YES
Distance (mm)	34.87	1.74	YES
Average Right and Left Height (mm)	475.87	0.42	YES
Average Right and Left Depth (mm)	478.98	0.30	YES

*All TEM values are less than 5% of the mean value for each particular trait.

Table 4.2: Intra-class Correlation Coefficient Non-Metric Measurements

	Intra-class Correlation	95% Confidence Interval		F Test with True Value 0			
		Lower Bound	Upper Bound	Value	df1	df2	Sig
Single Measure	0.998	0.996	0.998	882.032	98	98	0.000
Average Measure	0.999	0.998	0.999	882.032	98	98	0.000

Table 4.3: Intra-class Correlation Coefficient Metric Measurements

	Intra-class Correlation	95% Confidence Interval		F Test with True Value 0			
		Lower Bound	Upper Bound	Value	df1	df2	Sig
Single Measure	1.000	1.000	1.000	20639.229	98	98	.000
Average Measure	1.000	1.000	1.000	20639.229	98	98	.000

Non-Metric Characteristics

For non-metric evaluations, a p-value of ≤ 0.05 was considered statistically significant. No statistically significant differences were found between sexes in the frontal sinuses (χ^2 = 61.020; p-value = 0.473).

Shape of the Frontal Sinus in Anterior View—The quadrangle was the most common shape overall for both sinuses (27.38%). The quadrangle was the most common shape in both sinuses (32.26%) for males. The M-shape was the most common shape in the right sinus (27.27%) for females and the Fan-shape was the most common shape in the left sinus (36.36%) for females. For the right frontal sinus of males the following percentages of shapes were found: triangle (3%), right-angled triangle (16%), quadrangle (32.26%), parallelogram (0%), trapezoid (3%), fan-shaped (29.03%), M-shaped (0%), and crown (16.13%). For the right frontal sinus of females the following percentages of shapes were found: triangle (0%), right-angled triangle (18.18%), quadrangle (18.18%), parallelogram (0%), trapezoid (0%), fan-shaped (18.18%), M-shaped (27.27%), and crown (18.18%). For the left frontal sinus of males the following percentages of shapes were found: triangle (3%), right-angled triangle (6.45%), quadrangle (32.26%), parallelogram (6.45%), trapezoid (12.9%), fan-shaped (19.35%), M-shaped (6.68%), and crown (6.68%). For the left frontal sinus of females the following percentages of shapes were found: triangle (9.09%), right-angled triangle (9.09%), quadrangle (9.09%), parallelogram (0%), trapezoid (18.18%), fan-shaped (36.36%), M-shaped (9.09%), and crown (9.09%) (Figure 4.1). The shape of the frontal sinus in anterior view showed no statistically significant difference between the right and left sides (χ^2 = 8.557; p-value = 0.286). The shape of the frontal sinus in anterior view also showed no statistically significant difference in the right sinus between males and females (χ^2 = 10.133; p-value = 0.119) or the left sinus between males and females (χ^2 = 4.190; p-value = 0.758).

Figure 4.1: Shape of the Frontal Sinus in Anterior View (unit: %)

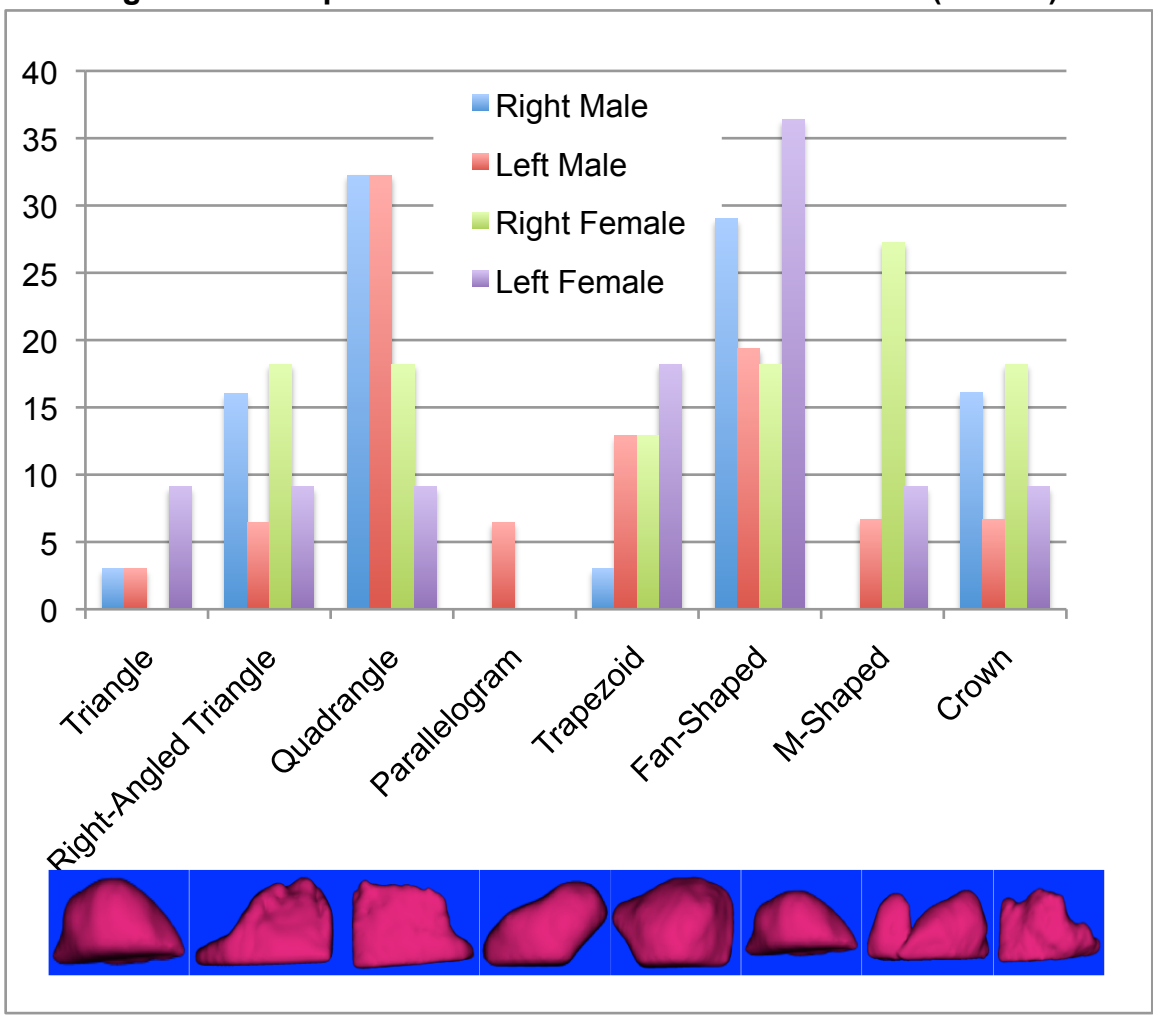

Shape of the Frontal Sinus in Lateral View—The concave shape was the most common overall for both sexes (53.57%). The concave shape was the most common in both sinuses (56.45%) for males. The flat (36.36%) and concave (36.36%) shapes were the most common in the right sinus for females. The concave shape was the most common in the left sinus (54.55%) for females. For the right frontal sinus of males the following percentage of shapes were found: flat (22.56%), convex (29.03%), and concave (48.39%). For the right frontal sinus of females the following percentage of shapes were found: flat (36.36%), convex (27.27%), and concave (36.36%). For the left frontal sinus of

males the following percentage of shapes were found: flat (9.68%), convex (25.81%), and concave (64.52%). For the left frontal sinus of females the following percentage of shapes were found: flat (18.18%), convex (27.27%), and concave (54.55%) (Figure 4.2). The shape of the frontal sinus in lateral view showed no statistically significant difference between the left and right sides (χ^2 = 3.382; p-value = 0.184). The shape of the frontal sinus in lateral view also showed no statistically significant difference in the right sinus between males and females (χ^2 = 0.857; p-value = 0.651) or the left sinus between males and females (χ^2 = 0.630; p-value = 0.730).

Figure 4.2: Shape of the Frontal Sinus in Lateral View (unit: %)

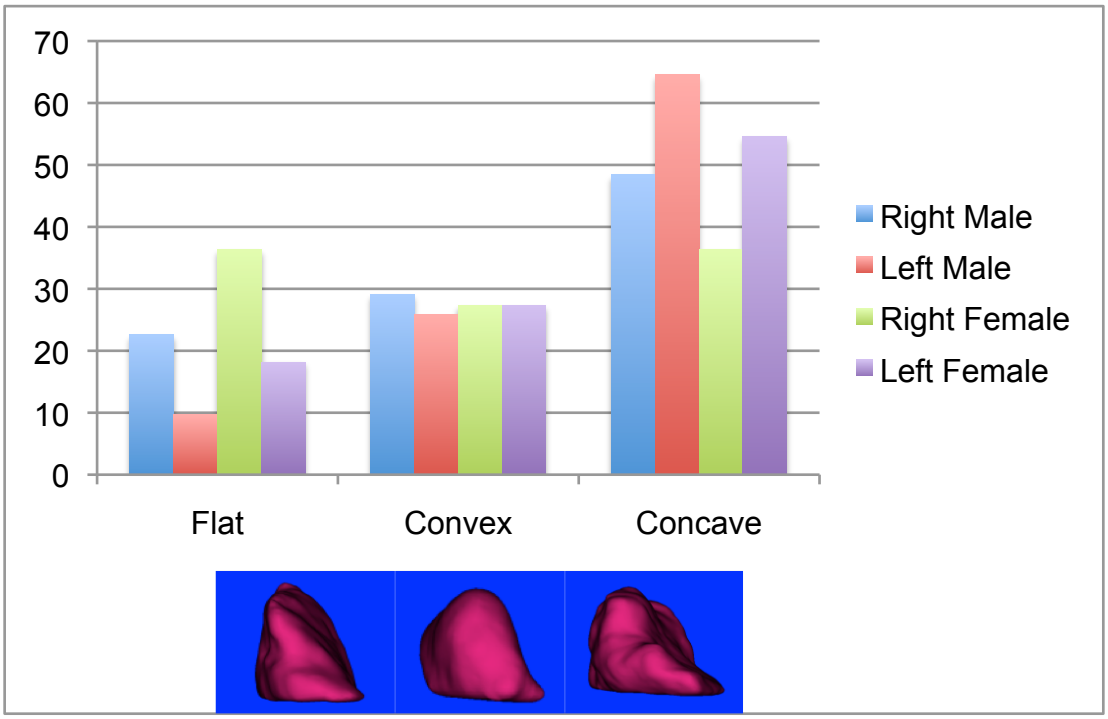

Outline of the Upper Border—A smooth outline (26.19%) and an outline of scallops with two arcades (26.19%) were the most common types overall for the right frontal sinus. A flat outline (23.81%) and an outline of scallops with two arcades (23.81%) were the most common types overall for the left frontal sinus.

A smooth outline (32.26%) was the most common type in the right sinus for males. An outline of scallops with two arcades (54.55%) was the most common type in the right sinus for females. A flat outline (32.26%) was the most common type in the left sinus for males. A smooth outline (36.36%) was the most common type in the left sinus for females. For the right frontal sinus in males the following percentages of outlines were found: flat (22.56%), smooth (32.26%), scallops with two arcades (16.13%), scallops with three arcades (12.9%), scallops with four arcades (9.68%), scallops with five arcades (6.45%), and scallops with six arcades (0%). For the right frontal sinus in females the following percentages of outlines were found: flat (18.18%), smooth (9.09%), scallops with two arcades (54.55%), scallops with three arcades (18.18%), scallops with four arcades (0%), scallops with five arcades (0%), scallops with six arcades (0%). For the left frontal sinus in males the following percentages of outlines were found: flat (32.26%), smooth (16.13%), scallops with two arcades (25.81%), scallops with three arcades (19.35%), scallops with four arcades (6.45%), scallops with five arcades (0%), and scallops with six arcades (0%). For the left frontal sinus in females the following percentages of outlines were found: flat (0%), smooth (36.36%), scallops with two arcades (18.18%), scallops with three arcades (18.18%), scallops with four arcades (9.09%), scallops with five arcades (9.09%), and scallops with six arcades (9.09%) (Figure 4.3). The outline of the upper border of the frontal sinus showed no statistically significant difference between the right and left sides (χ^2 = 1.919; p-value = 0.927). The outline of the upper border of the frontal sinus also showed no statistically significant difference

between the sexes in the right (χ^2 = 8.245; p-value = .143) and left (χ^2 = 11.019; p-value = 0.088) sinuses.

Figure 4.3: Outline of the Upper Border of the Frontal Sinus (unit: %)

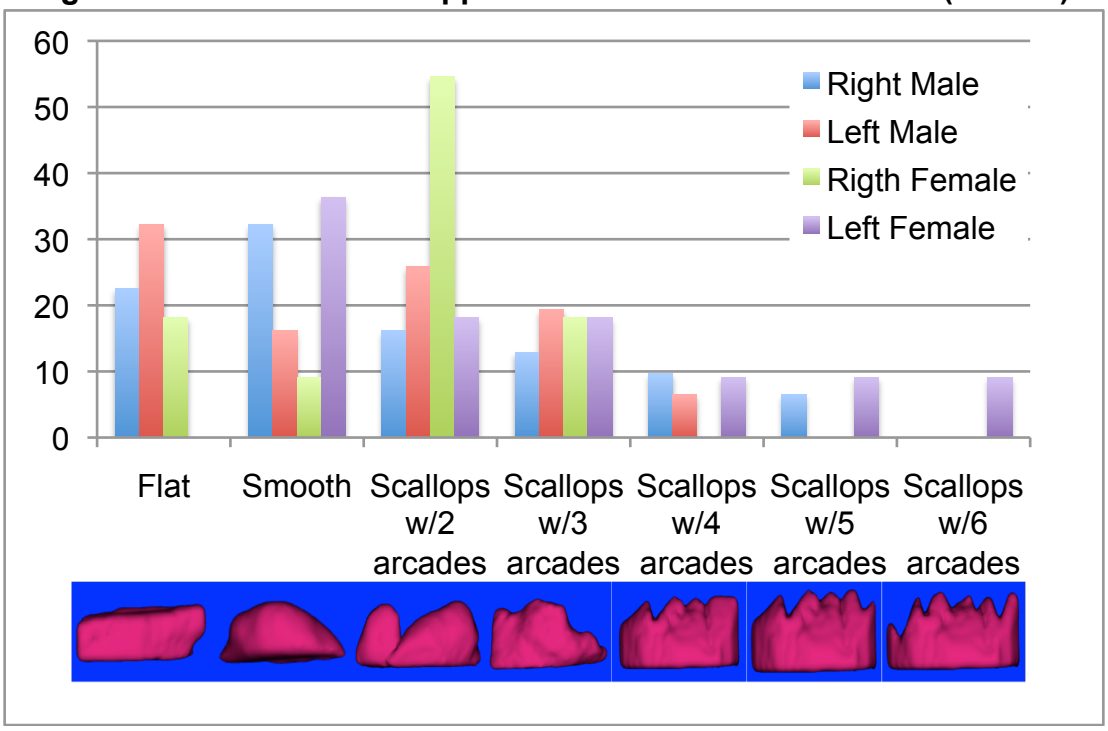

Cross-Sectional Shape—The most common cross-sectional shape overall for the right sinus was a crescent (42.86%) and a square (35.71%) for the left sinus. The crescent was the most common shape in the right sinus for males (32.26%) and females (72.73%). The square (38.71%) was the most common shape in the left sinus for males. The ellipse (36.36%) was the most common shape in the left sinus for females. For the right frontal sinus in males the following percentages of outlines were found: ellipse (29.03%), crescent (32.26%), square (25.81%), and irregular (12.9%). For the right frontal sinus in females the following percentages of outlines were found: ellipse (9.09%), crescent (72.73%), square (18.18%), and irregular (0%). For the left frontal sinus in males the following percentages of outlines were found: ellipse (19.35%),

crescent (19.35%), square (38.71%), and irregular (22.58%). For the left frontal sinus in females the following percentages of outlines were found: ellipse (36.36%), crescent (27.27%), square (27.27%), and irregular (9.09%) (Figure 4.4). The cross-sectional shape of the frontal sinus showed no statistically significant difference between the right and left sides (χ^2 = 5.333; p-value = 0.149). The cross-sectional shape of frontal sinus also showed no statistically significant difference between the sexes in the right (χ^2 = 6.076; p-value = 0.108) and left (χ^2 = 2.297; p-value = 0.513) sinuses.

Figure 4.4: Cross-Sectional Shape of the Frontal Sinus (unit: %)

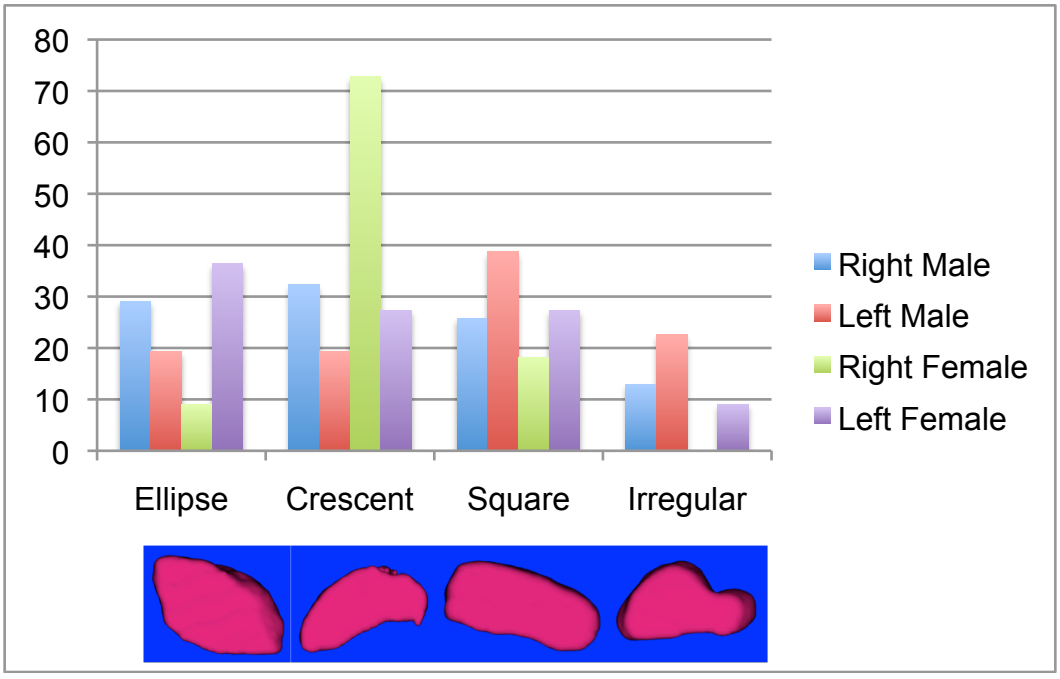

Metric Characteristics From the Baseline

A statistically significant difference was found between the sexes in the right depth using a two-sample *t*-test (p-value = 0.029) and Mann-Whitney *U* test (p-value = 0.0368). Though not statistically significant, the total volume, right volume, left volume, left width, right depth, left depth, right angle, and left angle

were all larger in males than in females (Table 4.4, Figure 4.5, Figure 4.6, and Figure 4.7). Though not statistically significant, the right width, distance, right height, and left height were all larger in females than in males (Table 4.4 and Figure 4.6).

Table 4.4: Metric Measurements from the Baseline of the Frontal Sinus (unit: mean [+/- standard deviation])

Measurements	Male	Female
Volume*		
Total	3761.77 +/- 4539.23	2969.41 +/- 3047.18
Right	1469.61 +/- 1060.19	1446.77 +/- 1525.8
Left	1664.66 +/- 1210.35	1522.64 +/- 1731.23
Only Right~	927.9	
Only Left~	1179.3	
Width		
Right	22.71 +/- 8.49	23.74 +/- 11.69
Left	23.3 +/- 7.08	19.31 +/- 7.99
Distance	24.75 +/- 14.19	29.73 +/- 11.94
Height		
Right	11.69 +/- 4.36	11.71 +/- 6.25
Left	12.32 +/- 3.96	12.83 +/- 7.14
Depth		
Right	11.98 +/- 2.87	9.92 +/- 2.36
Left	11.81 +/- 3.03	9.73 +/- 3.0
Angle+		

Right	111.65 +/- 23.97	85.15 +/- 24.83
Left	108.7 +/- 25.39	108.55 +/- 22.42

*Unit is mm^3
+Unit is °
~Single individual, no mean or standard deviation available.

Figure 4.5: Volume Mean Values from the Baseline (unit: mm^3)

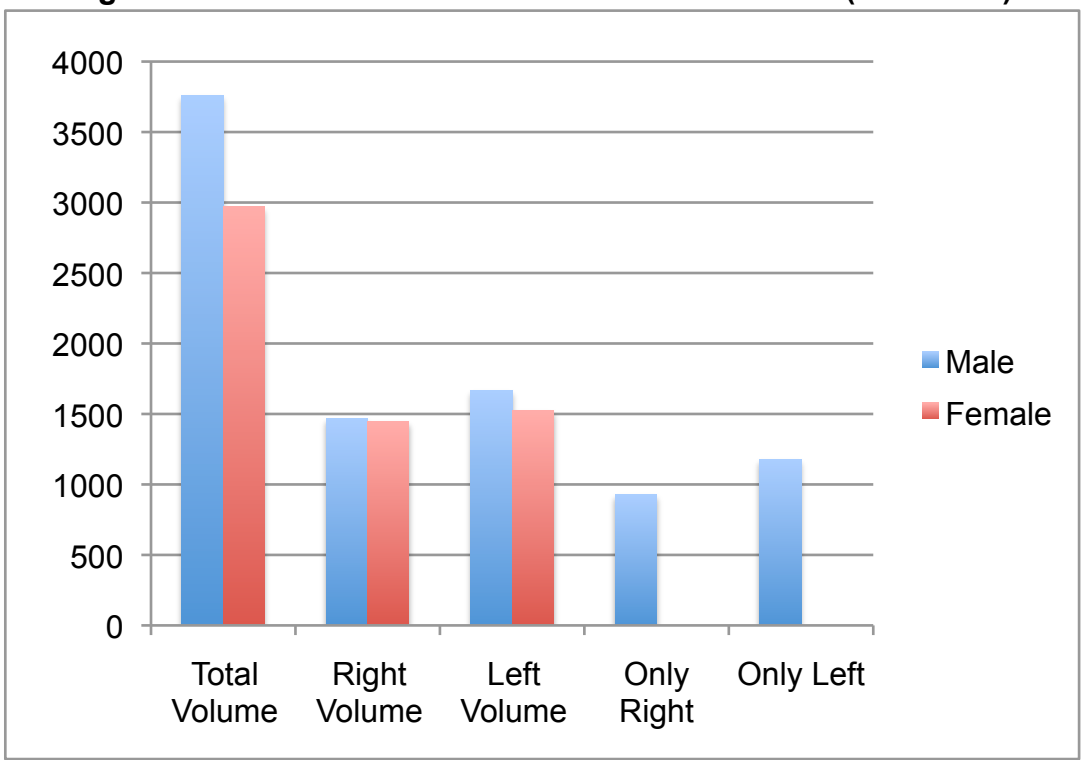

Figure 4.6: Width, Distance, Height, and Depth Mean Values from the Baseline (unit: mm)

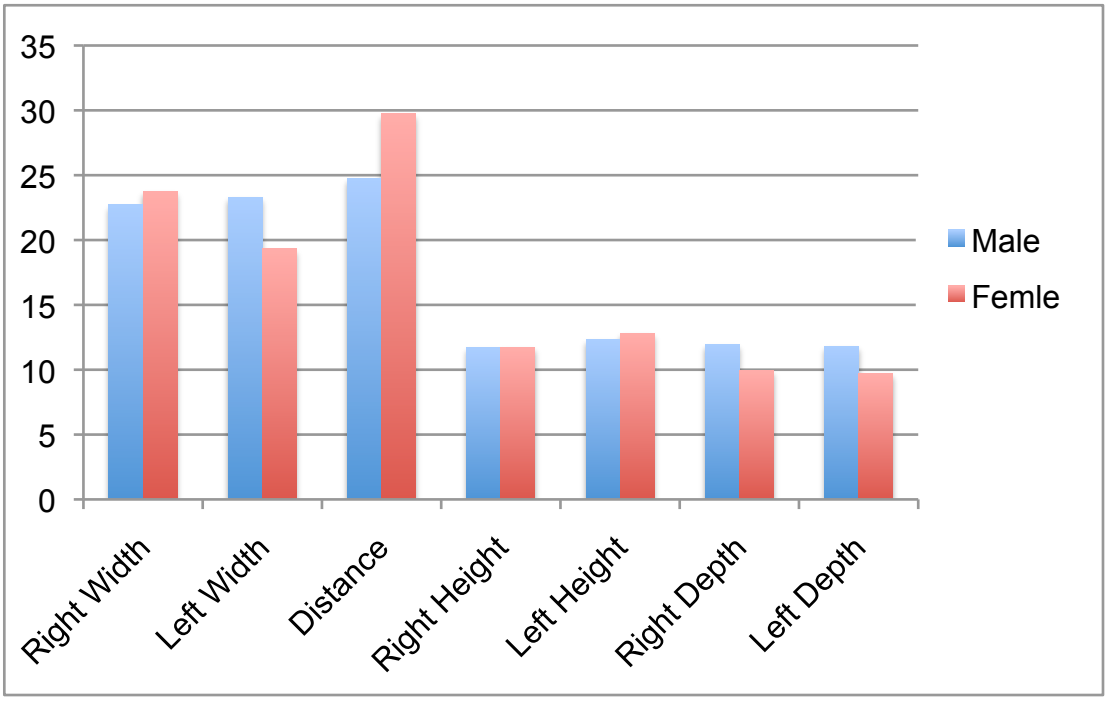

Figure 4.7: Angle Mean Values from the Baseline (unit: º)

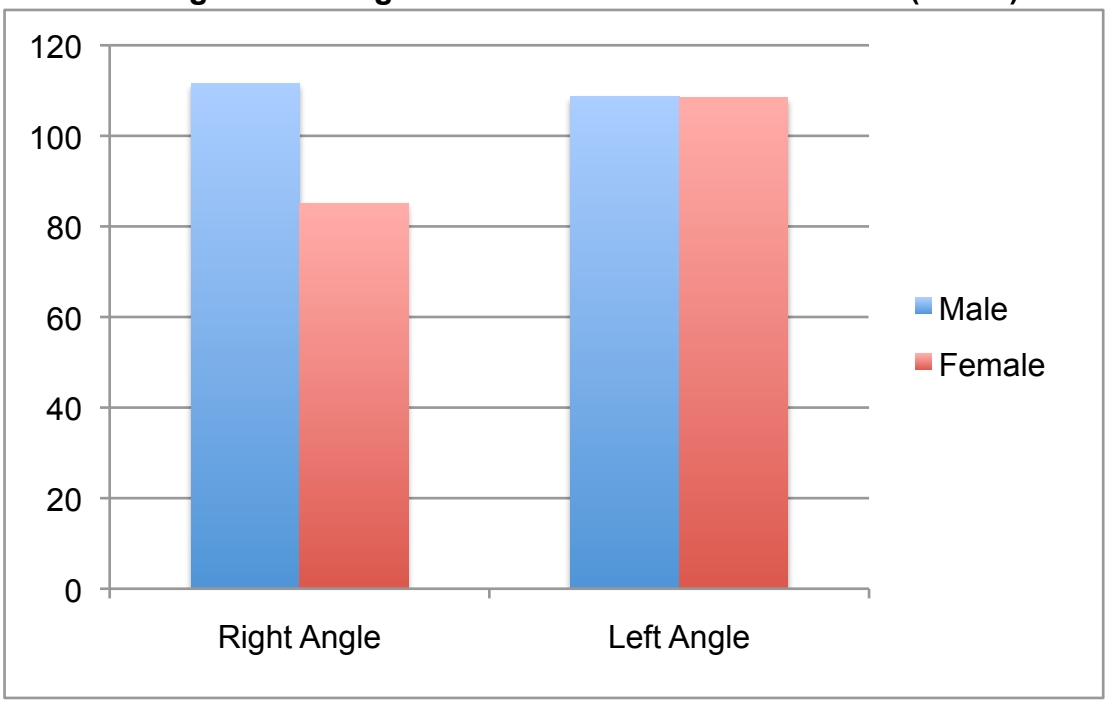

Volume—The total volume showed no statistically significant difference between the sexes (*t*-test p-value = 0.522; Mann-Whitney p-value = 0.5873).

The right volume showed no statistically significant difference between the sexes (*t*-test p-value = 0.964; Mann-Whitney p-value = 0.6274). The left volume showed no statistically significant difference between the sexes (*t*-test p-value = 0.806; Mann-Whitney p-value = 0.3167).

Width—The right width showed no statistically significant difference between the sexes (*t*-test p-value = 0.791; Mann-Whitney p-value = 0.7748). The left width showed no statistically significant difference between the sexes (*t*-test p-value = 0.162; Mann-Whitney p-value = 0.1908).

Distance—The distance showed no statistically significant difference between the sexes (*t*-test p-value = 0.272; Mann-Whitney p-value = 0.2770).

Height—The right height showed no statistically significant difference between the sexes (*t*-test p-value = 0.995; Mann-Whitney p-value = 0.7099). The left height showed no statistically significant difference between the sexes (*t*-test p-value = 0.826; Mann-Whitney p-value = 0.8783).

Depth—The right depth showed a statistically significant difference between the sexes (*t*-test p-value = 0.029; Mann-Whitney p-value = 0.0368). The left depth approached statistical significance between the sexes (*t*-test p-value = 0.064; Mann-Whitney p-value = 0.0683).

Complete Metric Characteristics

Statistically insignificant differences were found between males and females for complete frontal sinus measurements (not from the baseline). The total volume, right volume, left volume, and left width were all larger in males

than in females (Table 4.5, Figure 4.8, and Figure 4.9). The right width and distance were all larger in females than in males (Table 4.5 and Figure 4.9).

Table 4.5: Metric Measurements of the Complete Frontal Sinus (unit: mean [+/- standard deviation])

Measurements	Male	Female
Volume*		
Total	4984.98 +/- 2906.58	4322.18 +/- 3518.27
Right	2630.91 +/- 1555.02	2163.59 +/- 1825.91
Left	2528.65 +/- 1580.49	2158.59 +/- 2042.61
Only Right~	1738.3	
Only Left~	1859	
Width		
Right	23.27 +/- 7.78	24.05 +/- 11.43
Left	23.52 +/- 6.67	19.86 +/- 7.29
Distance	17.67 +/- 7.62	20.16 +/- 10.72
Height		
Right	20.07 +/- 6.23	17.41 +/- 4.89
Left	19.72 +/- 5.39	17.36 +/- 6.53

*Unit is mm^3

~Single individual, mean or standard deviation available.

Figure 4.8: Volume Mean Values of the Complete Frontal Sinus (unit: mm^3)

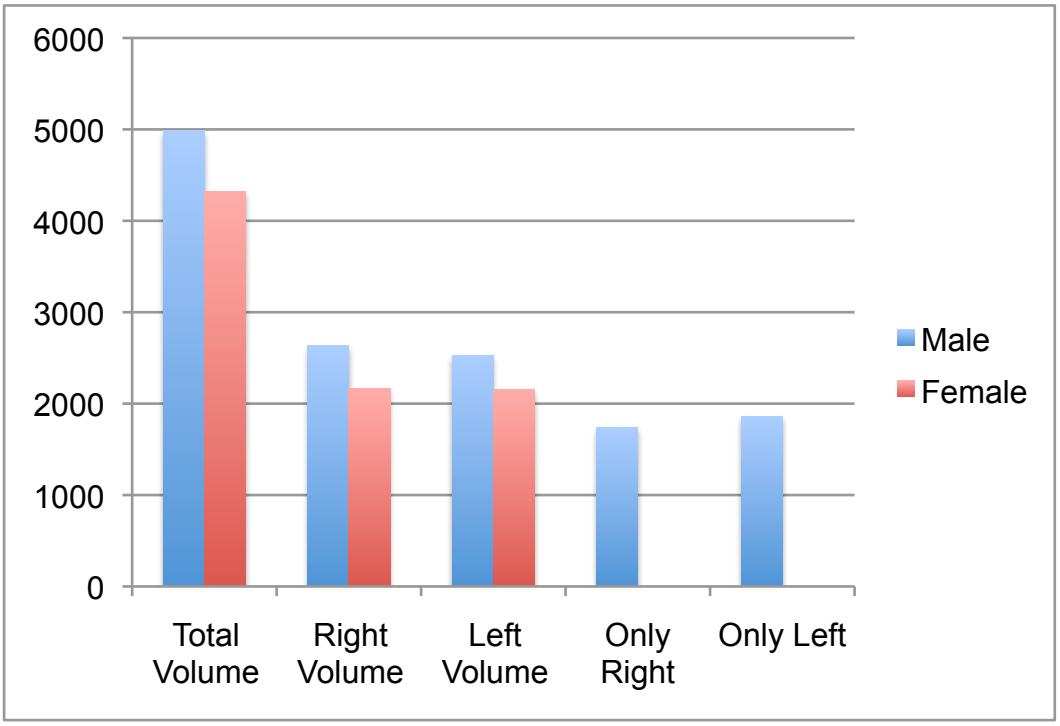

Figure 4.9: Width, Distance, and Height Mean Values of the Complete Frontal Sinus (unit: mm)

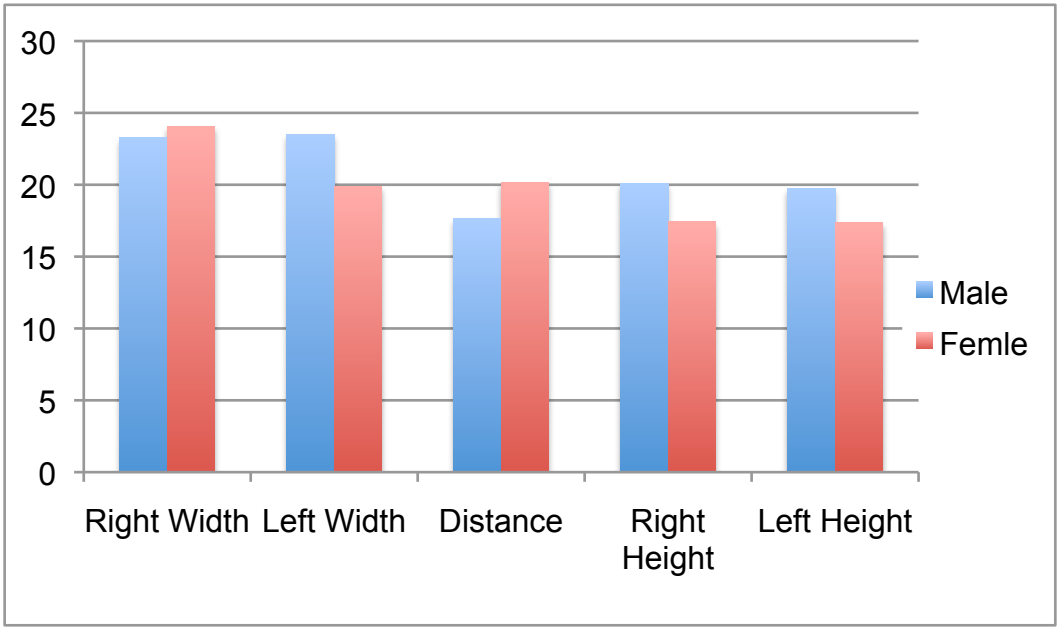

Volume—Total frontal sinus volume differences between the sexes failed to reach statistical significance (*t*-test p-value = 0.583; Mann-Whitney p-value = 0.3806). The right volume showed no statistically significant difference between

the sexes (*t*-test p-value = 0.461; Mann-Whitney p-value = 0.4231). The left volume showed no statistically significant difference between the sexes (*t*-test p-value = 0.594; Mann-Whitney p-value = 0.3167).

Width—The right width showed no statistically significant difference between the sexes (*t*-test p-value = 0.837; Mann-Whitney p-value = 0.7968). The left width showed no statistically significant difference between the sexes (*t*-test p-value = 0.162; Mann-Whitney p-value = 0.1908).

Distance—The distance showed no statistically significant difference between the sexes (*t*-test p-value = 0.492; Mann-Whitney p-value = 0.5868).

Height—The right height showed no statistically significant difference between the sexes (*t*-test p-value = 0.166; Mann-Whitney p-value = 0.2408). The left height showed no statistically significant difference between the sexes (*t*-test p-value = 0.299; Mann-Whitney p-value = 0.3231).

BAI and Angle

BAI—Table 4.6 illustrates the BAI when the frontal sinus was cut from the baseline. The most common type of BAI was "1 ($80 \leq$ BAI)" at 30.2% overall, 28.1% for males and 36.4% for females. No statistically significant difference between the sexes was found for the BAI ($\chi^2 = 2.690$; p-value = 0.748). Table 4.7 illustrates the BAI when the frontal sinus was not cut from the baseline. The most common type of BAI was "1 ($80 \leq$ BAI)" at 30.2% overall, 37.5% for males and 9.1% for females. The most common type of BAI for females was "4 ($20 \leq$ BAI < 40)" at 27.9%, 21.9% for males and 45.5% for females. No statistically

significant difference was found between the sexes for the BAI (χ^2 = 10.486; p-value = 0.063).

Table 4.6: Classification of the Frontal Sinus by Bilateral Asymmetry Index* (BAI) Using Volume (unit: %[n])

Class Number	Range Asymmetry Index	Males	Females	Total
B	Bilateral absence	0 (0)	0 (0)	0 (0)
U	Unilateral absence	6.3 (2)	0 (0)	4.7 (2)
1	80 ≤ BAI	28.1 (9)	36.4 (4)	30.2 (13)
2	60 ≤ BAI < 80	18.8 (6)	9.1 (1)	16.3 (7)
3	40 ≤ BAI < 60	15.6 (5)	9.1 (1)	13.9 (6)
4	20 ≤ BAI < 40	12.5 (4)	27.3 (3)	16.3 (7)
5	BAI < 20	18.8 (6)	18.2 (2)	18.6 (8)
F	Fused	0 (0)	0 (0)	0 (0)
M	Prominent middle	0 (0)	0 (0)	0 (0)

*Cut from baseline

Table 4.7: Classification of the Complete Frontal Sinus by Bilateral Asymmetry Index (BAI) Using Volume (unit: %[n])

Class Number	Range Asymmetry Index	Males	Females	Total
B	Bilateral absence	0 (0)	0 (0)	0 (0)
U	Unilateral absence	6.3 (2)	0 (0)	4.7 (2)
1	80 ≤ BAI	37.5 (12)	9.1 (1)	30.2 (13)
2	60 ≤ BAI < 80	25 (8)	18.2 (2)	23.3 (10)
3	40 ≤ BAI < 60	3.1 (1)	27.3 (3)	9.3 (4)
4	20 ≤ BAI < 40	21.9 (7)	45.5 (5)	27.9 (12)

5	BAI < 20	6.3 (2)	0 (0)	4.7 (2)
F	Fused	0 (0)	0 (0)	0 (0)
M	Prominent middle	0 (0)	0 (0)	0 (0)

Angle—The most common category of angle overall for both sexes was the category "less than 100°" (34.88%). The category "less than 100°" was also the most common in the right (28.13%) and left (34.38%) sinuses for males. The category "less than 100°" was the most common for females for the right frontal sinus (63.63%) and the category "100° to 109°" was the most common for the left frontal sinus (36.36%). The angle showed no statistically significant difference between the right and left sides (χ^2 = 2.789; p-value = 0.835). The angle showed no statistically significant difference between males and females in the right sinus (χ^2 = 7.872; p-value = 0.248) or the left sinus (χ^2 = 7.005; p-value = 0.320).

Combined Metric and Non-Metric Results

The Principal Components Analysis (PCA) suggests that sex may be influencing some of the variables. PC1 explains 33.6% of the variance, PC2 explains 11.9% of the variance, and PC3 explains 8.7% of the variance. Overlap in the data is shown for males and females along PCs 1-3 (Figure 4.10 and Figure 4.11). However, there is slight separation along PC2, with males lying along the negative end of this axis and females falling along the positive end of this axis. Values weighted most heavily along the positive end of PC2 where females lie include right side volume (0.203), right side width (0.340), complete right side volume (0.222), and complete right side width (0.347). Values weighted most heavily along the negative end of axis two where males lie include

left side width (-0.266), left side depth (-0.241), cross-sectional shape right (-0.363) complete left side width (-0.286), and complete left side height (-0.242). Based on the PCA analyses, these variables contribute most to differences between males and females along PC2.

The weight for the variables PC2 are as follows: total volume (0.291), right side volume (0.270), left side volume (0.271), right side width (0.192), left side width (0.219), distance (0.105), right side height (0.245), left side height (0.198), right side depth (0.199), left side depth (0.153), right side angle (0.067), left side angle (-0.055), anterior view right (0.020), anterior view left (-0.033), lateral view right (-0.114), lateral view left (0.040), outline of upper border right (-0.041), outline of upper border left (-0.033), cross-sectional shape right (0.054), cross-sectional shape left (0.123), bilateral asymmetry index (-0.158), complete total volume (0.304), complete right side volume (0.270), complete left side volume (0.280), complete right side width (0.186), complete left side width (0.216), complete distance (0.100), complete right side height (0.207), complete left side height (0.176), and complete bilateral asymmetry index (-0.181).

The weight for the variables of PC2 are as follows: total volume (0.038), right side volume (0.203), left side volume (-0.112), right side width (0.340), left side width (-0.266), distance (0.129), right side height (0.145), left side height (-0.105), right side depth (-0.007), left side depth (-0.241), right side angle (-0.080), left side angle (0.188), anterior view right (0.177), anterior view left (0.033), lateral view right (0.024), lateral view left (0.014), outline of upper border right (0.120), outline of upper border left (0.199), cross-sectional shape right (-0.363),

cross-sectional shape left (0.053), bilateral asymmetry index (0.027), complete total volume (0.060), complete right side volume (0.222), complete left side volume (-0.106), complete right side width (0.347), complete left side width (-0.286), complete distance (0.173), complete right side height (0.074), complete left side height (-0.242), and complete bilateral asymmetry index (0.165).

The weight for the variables for PC3 are as follows: total volume (-0.053), right side volume (0.014), left side volume (-0.105), right side width (0.156), left side width (-0.123), distance (0.024), right side height (0.007), left side height (-0.301), right side depth (0.170), left side depth (-0.029), right side angle (0.019), left side angle (-0.095), anterior view right (-0.341), anterior view left (-0.285), lateral view right (-0.306), lateral view left (-0.142), outline of upper border right (-0.384), outline of upper border left (-0.376), cross-sectional shape right (0.194), cross-sectional shape left (-0.009), bilateral asymmetry index (0.028), complete total volume (-0.005), complete right side volume (0.103), complete left side volume (-0.109), complete right side width (0.172), complete left side width (-0.117), complete distance (-0.150), complete right side height (0.123), complete left side height (-0.244), and complete bilateral asymmetry index (-0.119).

Figure 4.10: Principal Components Analysis (PCA) Axis 1 and Axis 2

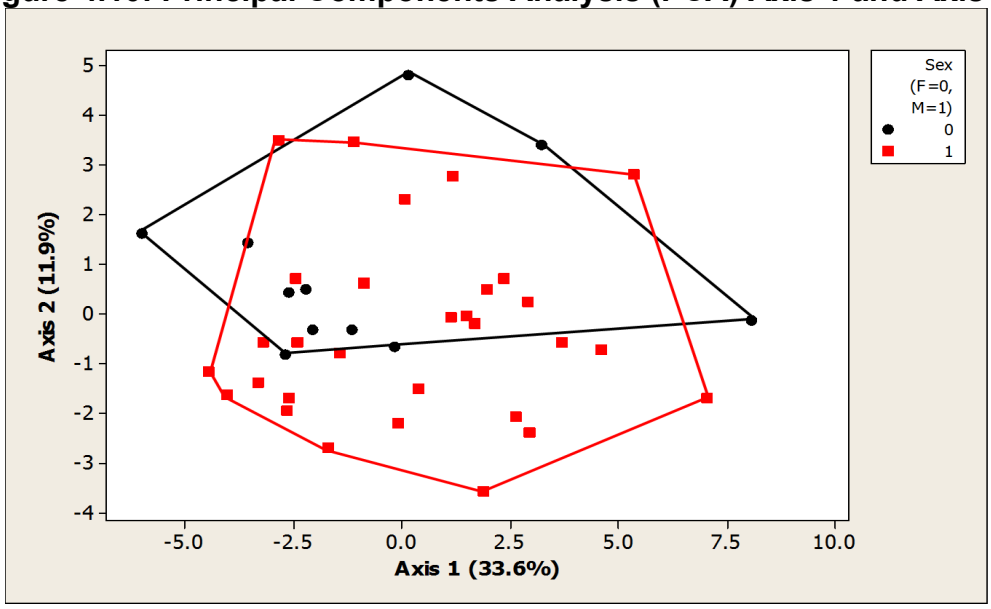

Figure 4.11: Principal Components Analysis (PCA) Axis 2 and Axis 3

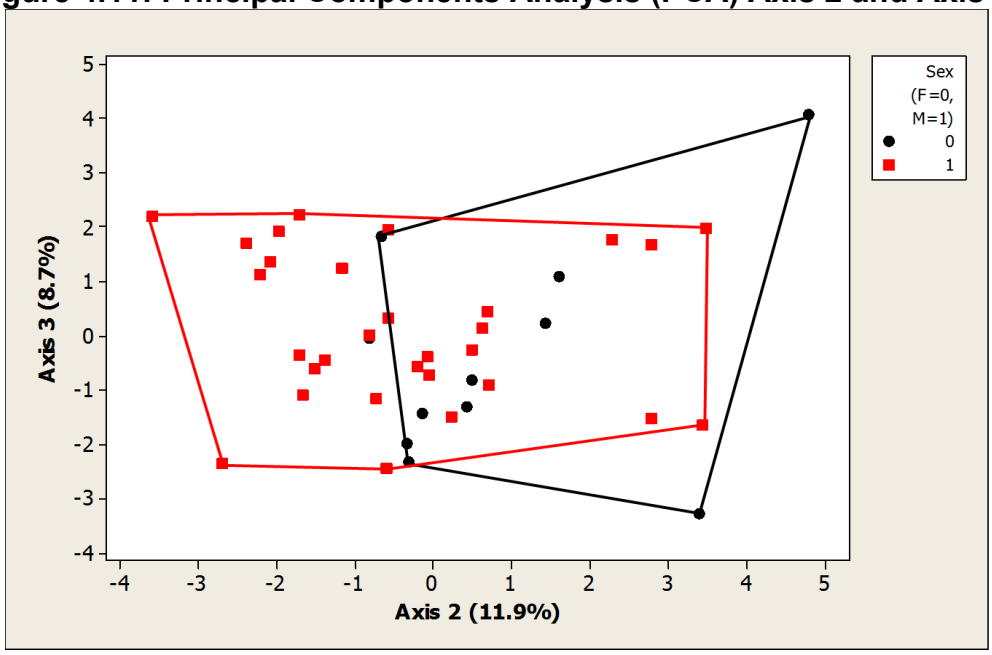

Digit Code Results

A total of 43 frontal sinuses, 32 males and 11 females, were evaluated for potential differences in frontal sinus configuration of non-metric characteristics and a digit code was created. The digit codes, composed of six sections and an

eleven-digit number, were able to accurately identify individuals 100% of the time (Table 4.8). No two digit codes were shown to be identical.

Table 4.8: Digit Codes

Individual #	From Baseline	Not From Baseline
1	1/33/13/20/CC/14	4/33/13/20/CC/14
2	4/27/22/12/EI/34	3/27/22/12/EI/34
3	1/68/23/33/CS/32	1/68/23/33/CS/32
4	5/66/22/21/SS/11	2/66/22/21/SS/11
5	5/66/33/33/EC/22	5/66/33/33/EC/22
6	1/65/23/13/EE/74	1/65/23/13/EE/74
7	2/33/22/01/SC/55	2/33/22/01/SC/55
9	1/88/13/36/CS/13	3/88/13/36/CS/13
10	3/82/33/52/CS/53	1/82/33/52/CS/53
12	4/25/13/21/CS/14	4/25/13/21/CS/14
13	2/85/32/30/CS/51	2/85/32/30/CS/51
14	4/65/12/00/CS/24	4/65/12/00/CS/24
15	3/26/31/25/CC/11	3/26/31/25/CC/11
16	3/56/33/11/ES/43	2/56/33/11/ES/43
17	4/86/23/22/CC/22	4/86/23/22/CC/22
18	3/13/21/10/SC/23	1/13/21/10/SC/23
19	1/35/23/01/SS/11	2/35/23/01/SS/11
20	1/27/33/22/IC/11	2/27/33/22/IC/11
21	5/81/33/01/CE/46	4/81/33/01/CE/46
23	5/33/12/01/CE/22	4/33/12/01/CE/22
24	2/34/23/44/SC/36	2/34/23/44/SC/36
26	5/61/22/31/CE/14	4/61/22/31/CE/14
27	4/72/33/24/CC/17	3/72/33/24/CC/17
28	5/64/23/12/EI/41	4/64/23/12/EI/41
30	3/33/13/00/SC/51	1/33/13/00/SC/51
31	1/35/33/42/CS/13	1/35/33/42/CS/13
32	1/62/33/12/ES/12	1/62/33/12/ES/12
33	2/33/11/00/SS/61	1/33/11/00/SS/61
35	3/33/13/00/SI/21	1/33/13/00/SI/21
36	5/28/32/23/II/25	4/28/32/23/II/25
38	1/63/31/50/II/11	2/63/31/50/II/11
39	1/77/31/22/CE/11	4/77/31/22/CE/11
41	4/27/31/22/CE/61	4/27/31/22/CE/61
42	U/6N/3N/2N/EN/4N	U/6N/3N/2N/EN/4N
43	1/76/33/23/EE/42	1/76/33/23/EE/42
44	2/26/33/11/EE/13	2/26/33/11/EE/13
45	U/N6/N2/N1/NE/N4	U/N6/N2/N1/NE/N4
46	1/33/13/00/ES/11	1/33/13/00/ES/11
47	4/88/32/44/CS/35	4/88/32/44/CS/35

48	5/83/33/30/IC/52	5/83/33/30/IC/52
49	1/36/33/13/CC/13	1/36/33/13/CC/13
50	2/66/12/13/SE/22	2/66/12/13/SE/22
51	2/33/12/10/SS/31	1/33/12/10/SS/31

Digit Code Comparison Results

After all of the measurements were taken and the digit codes were created, five individuals from the sample were then measured a second time while blinded to their identity and previous results. These measurements were then used to create their own unique digit codes. Once this was done, these new digit codes were matched to the previous sample while still blinded to the individuals (Table 4.9). This allowed for the evaluation of the usefulness for actually identifying an individual from the proposed digit code method. All five of these comparison digit codes were matched to the original sample with 100% accuracy.

Table 4.9: Digit Code Comparison

Blinded Digit Code	Matched Digit Code	Individual #
1/76/33/23/EE/42	1/76/33/23/EE/42	43
1/35/33/42/CS/13	1/35/33/42/CS/13	31
5/66/33/33/EC/22	5/66/33/33/EC/22	5
1/36/33/13/CC/13	1/36/33/13/CC/13	49
1/27/33/22/IC/11	1/27/33/22/IC/11	20

Chapter Five – Discussion and Conclusions

The forensic identification of unknown individuals is a crucial task faced by forensic anthropologists and it is a long-standing goal in the field to consistently seek improved methods for meeting this challenge. Forensic anthropologists are well versed in methods of positive identification of human skeletal remains; however, few studies have evaluated the usefulness of 3D CBCT images of the frontal sinus for the purpose of making a positive identification (Christensen 2004; Jablonski and Shum 1989; Steadman et al. 2006). Currently, there are no agreed upon standards for the objective comparison of the frontal sinus with known error rates (Cox et al. 2009). In 1925, Culbert and Law used the frontal sinus to identify human remains by comparing antemortem and postmortem radiographs (Reichs 1993). Since this time, radiographs have been used for the positive identification of human skeletal remains. However, it has been shown that there are potential problems with using 2D radiographs to evaluate the frontal sinuses (Christensen 2004; Kim et al. 2013; Reichs 1993). CT and CBCT are much better tools for analysis than radiographs because they allow for increased visualization of the internal structure of the sinus in greater detail. 3D CBCT is both accurate and reliable as a standard method of anthropometric measurement and has the ability to greatly improve upon current methods of positive identification (Guijarro-Martinez and Swennen 2013; Fourie et al. 2011).

The purpose of this study was to evaluate a standardized approach to identification using the frontal sinus that complies with the criteria outlined in *Daubert* for admissibility of scientific evidence. This study retrospectively

reviewed 3D CBCT scans of a total of 43 Caucasian patients, ages 20-38, from the Indiana University School of Dentistry in an attempt to identify individuals from frontal sinus comparisons, as well as analyze any significant differences between the frontal sinuses of adult males and females. This study replicated methods used in Kim, et al. (2013) to determine if their proposed method for identification was useful and accurate and to assess actual error values. Non-metric and metric data were analyzed and an eleven-digit code was made to test the uniqueness of each frontal sinus. It was observed that the frontal sinus had considerable individual variation (e.g. mean values, standard deviations, and non-metric values), which could lead to a positive identification.

Research Questions Reviewed

It was shown that 3D CBCT images of the frontal sinus could be used to make a positive forensic identification. Metric measurements displayed a high degree of variability between sinuses and no two digit codes in this small sample were identical. On the other hand, it was also shown that there were relatively few quantifiable and significant sexually dimorphic differences between male and female frontal sinuses. The depth of the right frontal sinus was the only measurement, metric or non-metric, that had a statistically significant difference between the sexes using univariate statistical tests ($p \leq 0.05$). It remains to be seen if this difference would hold up in a study involving a larger sample size. It is also possible that with a larger sample size other values would reach significance between the sexes. Most values were larger in males than in females, including the total volume, right volume, left volume, left width, right

depth, left depth, right angle, and left angle, as can be seen in Tables 4.4-4.10. It has been suggested that the high inter-individual variability of the frontal sinus renders them of little value in sex determination (Cox et al. 2009; Goyal et al. 2012; Yoshino et al. 1987). The results from the Principal Components Analysis (PCA) suggested that sex may be slightly affecting some of the variables (Figure 4.10 and Figure 4.11). Overlap was seen for males and females in both Figure 4.10 and Figure 4.11, although a slight separation along PC2 is also seen. This could be related to the sample size, or may represent specific traits or outliers. While Kim, et al. (2013) reported a statistical difference between the sexes in their study of 119 Korean cadavers, many other reports have claimed the opposite (Belaldavar et al. 2014; Camargo et al. 2007; Goyal et al. 2012; Yoshino et al. 1987). This difference may be due to small sample sizes, or the specific population being studied. Both of these factors need to be taken into account when studying the usefulness of the frontal sinus for the purpose of identification.

The proposed methods suggested by Kim et al. (2013) proved to be possible without significant training and most of them were easy to replicate. However, Kim et al. (2013) did not give appropriate details on how they conducted all of their measurements. Along with this, they did not provide results from an error study nor did they consistently describe which statistics they used. While I originally hypothesized that a combined use of metric and non-metric methods could serve to strengthen current methods of analysis for personal identification using the frontal sinus, this research proved the opposite. The use of digit codes is good in theory; however, the measurements needed to produce

them are time-consuming and subjective. While I conducted an error study that produced 95% confidence intervals and I had low intra-observer error rate, the possibility of inter-observer error is high without uniform training and explicit definitions of measurements collected. The non-metric methods proposed by Kim et al. (2013) are not quantitative measurements that can hold up against the *Daubert* ruling. Depending on who is assessing a shape of a frontal sinus, very different conclusions may be reached due to differences in anatomical training and experience. The methods proposed by Kim et al. (2013) also involve cutting the frontal sinus from the baseline, which reduces individual variability of the inferior dimensions of the frontal sinuses.

The use of 3D CBCT imaging has much to offer the field of forensic anthropology and frontal sinus analysis. While current research and methods do not meet all of the requirements for the *Daubert* ruling, this technique could be easily improved upon in order to stand up in a court of law. Larger samples, more diverse samples, and cross-population samples should be studied in order to better evaluate frontal sinus variation. Although the use of multidimensional statistical analysis requires significant training and advanced software, the average person would not be performing this analysis. If the frontal sinus were to be used to identify unknown human remains, individuals with advanced training would do it. It is because of this that I recommend that future research focus on creating geometric morphometric techniques that use three-dimensional landmarks and multidimensional statistics to produce a more accurate comparison of the frontal sinus.

Conclusions

In conclusion, the proposed method by Kim et al. (2013) should not be used for forensic identification purposes. While the creation of a digit code may provide appropriate supplemental evidence of positive identification, a digit code alone is not reliable enough to accurately produce a positive identification. It does not follow the standards set up by the *Daubert* ruling and when used in a larger sample, duplicate digit codes may be produced. A standardized method of analysis needs to be created which uses metric measurements of the frontal sinuses that are precisely defined using anatomical terminology.

As indicated in the present study, the use of 3D CBCT imaging has much to offer frontal sinus analysis. More accurate and replicable measurements can be taken, including volume, height, width, and depth of the frontal sinuses. This study also largely confirms research that suggests that sex determination should not be a primary goal of frontal sinus analysis. It is my hope that this research will highlight the importance of creating a standard method of frontal sinus analysis based on metric measurements; that conforms to *Daubert* standards and has the ability to accurately identify unknown human skeletal remains.

Chapter Six – Appendices

6.1 – Two-Sample *t*-Test of Right Depth

Two-Sample T-Test and CI: Right Depth, Sex

```
Two-sample T for Right Depth

Sex   N   Mean  StDev  SE Mean
0    11   9.92   2.36     0.71
1    31  11.97   2.87     0.51


Difference = mu (0) - mu (1)
Estimate for difference:  -2.056
95% CI for difference:  (-3.883, -0.228)
T-Test of difference = 0 (vs not =): T-Value = -2.34  P-Value = 0.029  DF = 21
```

6.2 – Alignment of Images

6.2a – Vertical Alignment of 3D CBCT Scan

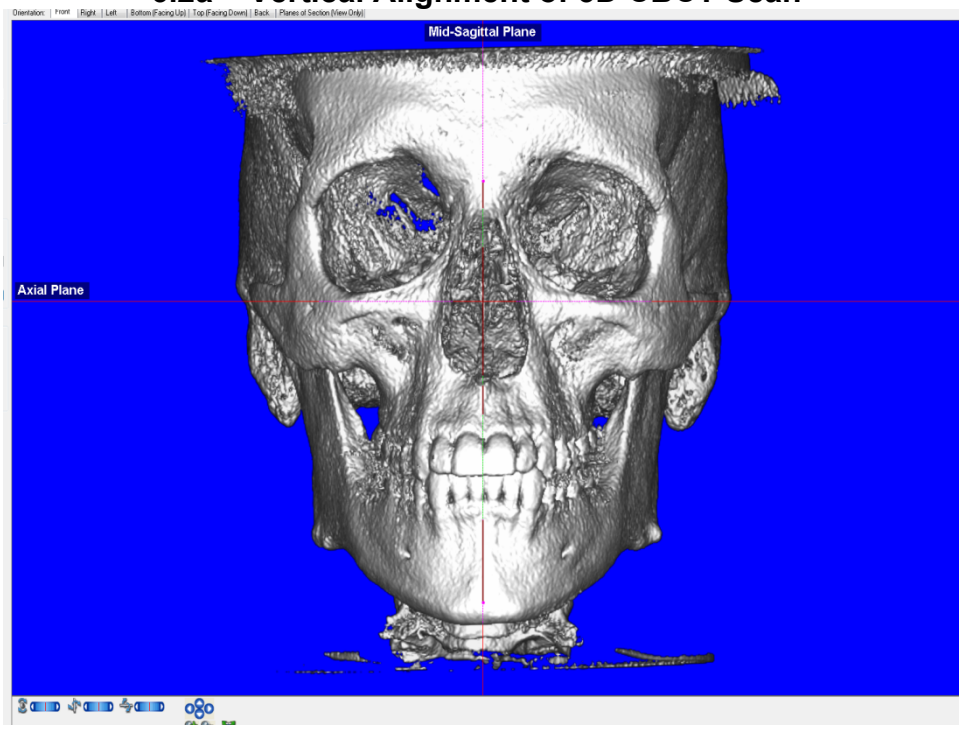

6.2b – Horizontal Alignment of 3D CBCT Scan

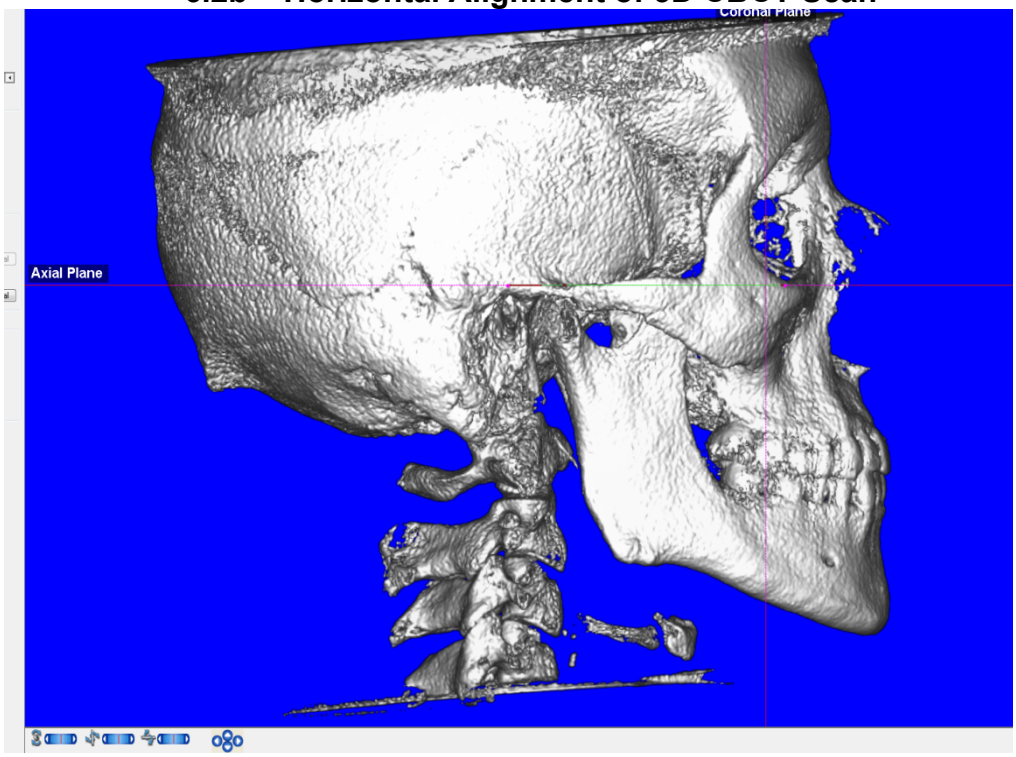

6.3 – 3D Images of the Frontal Sinus

6.3a – Outline of Frontal Sinus in Dolphin Imaging Software

6.3b— View of Frontal Sinus with Airways

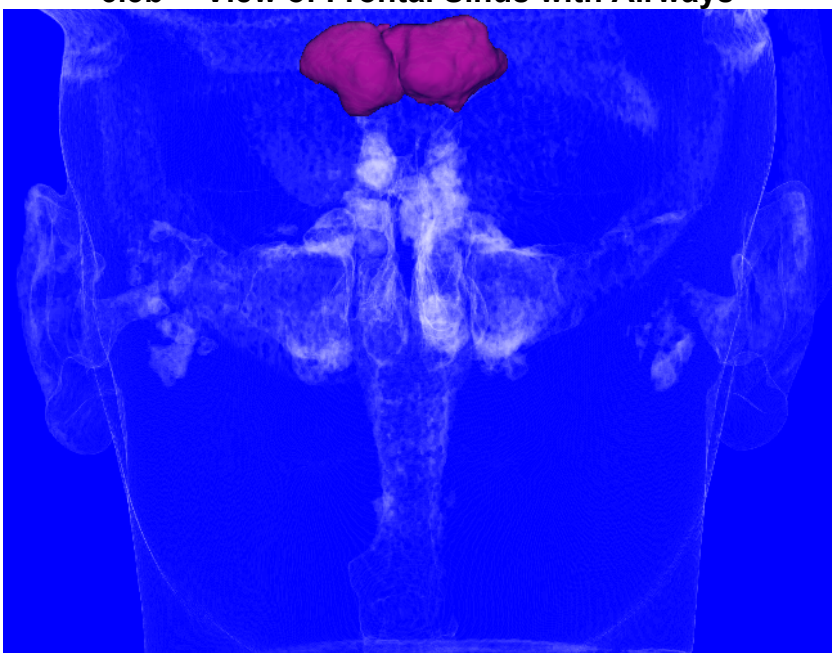

6.3c – View of the Frontal Sinus with Hard Tissue

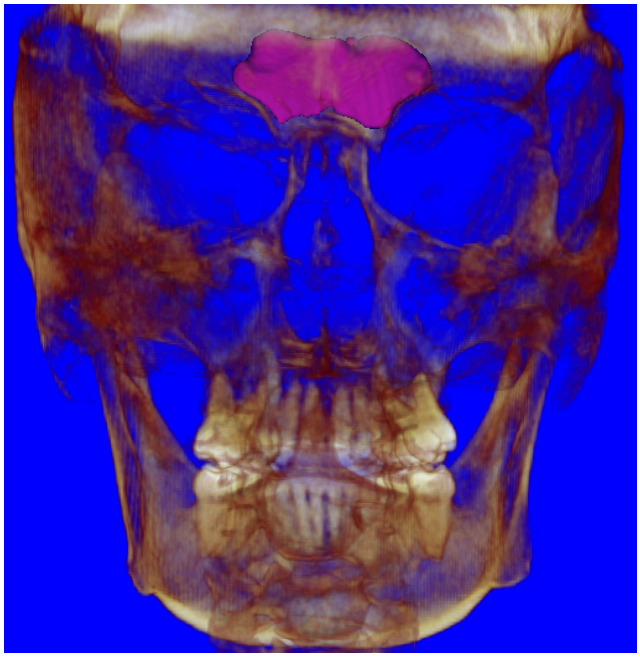

6.3d – 3D Rendering of Frontal Sinus

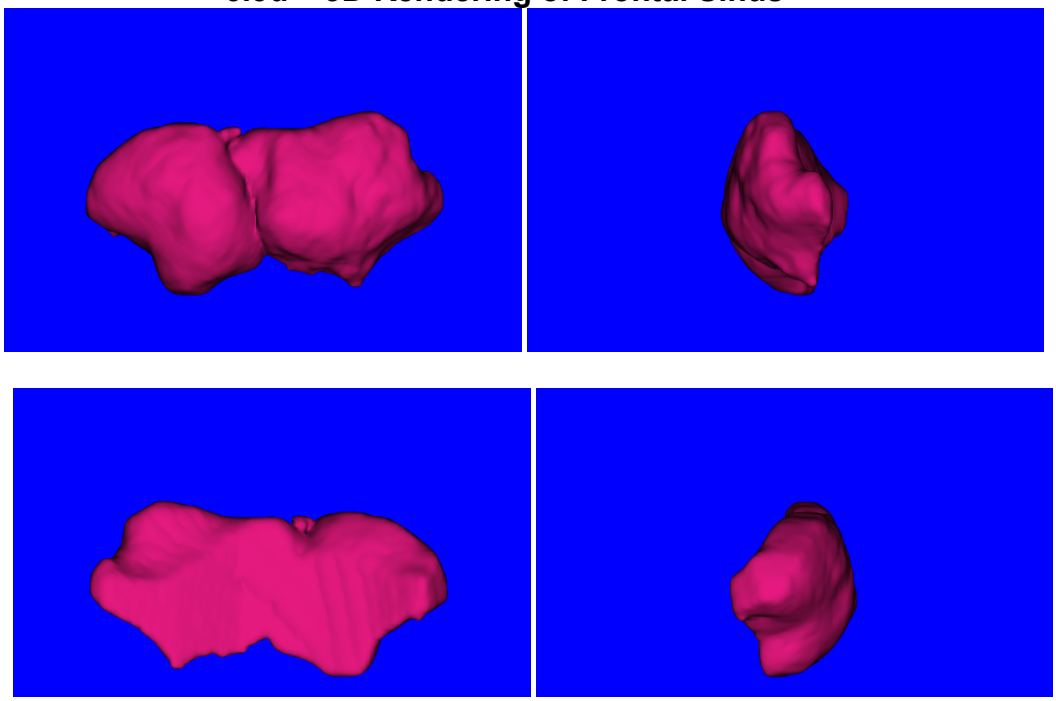

6.4 – Variation Lost by Cutting from the Baseline

References

Beladlavar, Chetan, Vijayalakshmi S. Kotrashetti, Seema R. Halikerimath, and Alka D. Kale

2014 Assessment of the Frontal Sinus Dimensions to Determine Sexual Dimorphism Among Indian Adults. Journal of Forensic Dental Sciences 6(1):25-31.

Camargo, JR., E. Daruge, FB. Prado, PHF. Caria, MC. Alves, RF. Silva, and E. Daruge Jr.

2007 The Frontal Sinus Morphology in Radiographs of Brazilian Subjects: Its Forensic Importance. Brazilian Journal of Morphological Science 24(4):239-243.

Cameriere, Roberto, Luigi Ferrante, Theya Molleson, and Barry Brown

2008 Frontal Sinus Accuracy in Identification as Measured by False Positives in Kin Groups. Journal of Forensic Science 53(6):1-3.

Christensen, Angi M.

2004 Assessing the Variation in Individual Frontal Sinus Outlines American Journal of Physical Anthropology 127(1):291-295.

Cox, Mary, Matthew Malcolm, and Scott I. Fairgrieve

2009 A New Digital Method for the Objective Comparison of Frontal Sinuses for Identification. Journal of Forensic Science 54(4):761-772.

Dirkmaat, Dennis C., Luis L. Cabo, Stephen D. Ousley, and Steven A. Symes

2008 New Perspectives in Forensic Anthropology. Yearbook of Physical Anthropology 51(1):33-52.

Fourie, Zacharias, Janalt Damstra, Peter O. Gerrits, and Yyijin Ren

2011 Evaluation of Anthropometric Accuracy and Reliability Using Different Three-Dimensional Scanning Systems. Forensic Science International 207(1):127-134.

Goyal, Megha, Ashith B. Acharya, Atul P. Sattur, and Venkatesh G. Nalkmasur

2012 Are Frontal Sinuses Useful Indicators of Sex? Journal of Forensic and Legal Medicine 20(1):91-94.

Guijarro-Martinez, R. and G. R. J. Swennen

2013 Three-Dimensional Cone Beam Computed Tomography Definition of the Anatomical Subregions of the Upper Airway: A Validation Study. International Journal of Oral & Maxillofacial Surgery 42(1):1140-1149.

Harris, Edward F. and Richard N. Smith
2008 Accounting for Measurement Error: A Critical But Often Overlooked Process. Archives of Oral Biology 54S(1):S107-S117.

Jablonski, Nina G. and Bobby S.F. Shum
1989 Identification of Unknown Human Remains by Comparison of Antemortem and Postmortem Radiographs. Forensic Science International 42(1):221-230.

Keierleber, J. A. and T. L. Bohan
2005 Ten Years After Daubert: The Status of the States. Journal of Forensic Science 50(1):1154-63.

Kim, Ddeog-Im, U-Young Lee, Sang-Ouk Park, Dae-Soon Kwak, and Seung-Ho Han
2013 Identification Using Frontal Sinus by Three-Dimensional Reconstruction from Computed Tomography. Journal of Forensic Science 58(1):5-12.

Nambiar, Phrabhakaran, Murali D.K. Naidu, and Krishnan Subramaniam
1999 Anatomical Variability of the Frontal Sinuses and Their Application in Forensic Identification. Clinical Anatomy 12(1):16-19.

Pfaeffli, Matthias, Peter Vock, Richard Dirnhofer, Marcel Braun, Stephan A. Bolliger, and Michael J. Thali
2007 Post-Mortem Radiological CT Identification Based on Classical Ante-Mortem X-ray Examinations. Forensic Science International 171(1):111-117.

Quatrehomme, Gerald, Pierre Fronty, Michel Sapanet, Gilles Grevin, Ppaul Bailet, and Amedee Ollier
1996 Identification by Frontal Sinus Pattern in Forensic Anthropology. Forensic Science International 83(1):147-153.

Reichs, Kathleen J.
1993 Quantified Comparison of Frontal Sinus Patterns by Means of Computed Tomography. Forensic Science International 61(1):141-168.

Schuller, A.
1943 A Note on the Identification of Skulls by X-ray Pictures of the Frontal Sinus. Med. Journal Australia 1(1):554-556.

Steadman DW, Adams BJ, Konigsberg LW
2006 Statistical Basis for Positive Identification in Forensic Anthropology. American Journal of Physical Anthropology 131:27-32.

Sutthiprapaporn P., K. Tanimoto, M. Ohtsuka, T. Nagasaki, Y. Iida, and A. Katsumata
2008 Positional Changes of Oropharyngeal Structures Due to Gravity in the Upright and Supine Positions. Dentomaxillofacial Radiology 37(1):130-5.

Tatlisumak, Ertugrul, Gulgun Yilmaz Ovali, Mahmut Asirdizer, Asim Aslan, Beyhan Oozyurt, Petek Bayindir, and Serdar Tarhan
2008 CT Study on Morphology of Frontal Sinus. Clinical Anatomy 21(1):287-293.

Tatlisumak, Ertugrul, Gulgun Yilmaz Ovali, Asim Aslan, Mahmut Asirdizer, Yildiray Zeyfeoglu, and Serdar Tarhan
2007 Identification of Unknown Bodies by Using CT Images of Frontal Sinus. Forensic Science International 166(1):42-48.

Tatlisumak, Ertugrul, Mahmut Asirdizer, and Mehmet Sunay Yavuz
2011 Usability of CT Images of Frontal Sinus in Forensic Personal Identification. Theory and Applications of CT Imaging and Analysis, Prof. Noriyasu Homma , ed. InTech Publishers.

Uthman, Asmaa T., Natheer H. AL-Rawi, Ahmed S. Al-Naaimi, Ahmed S. Tawfeeq, and Enas H. Suhail
2010 Evaluation of Frontal Sinus and Skull Measurements Using Spiral CT Scanning: An Aid in Unknown Person Identification. Forensic Science International 197(1):124.e1-124.e7.

Yoshino, Mineo, Sachio Miyasaka, Hajime Sato, and Sueshige Seta
1987 Classification System of Frontal Sinus Patterns by Radiography. Its Application to Identification of Unknown Skeletal Remains. Forensic Science International 34(1):289-299.

Curriculum Vitae
Bianaca S. Krus

EDUCATION

MA Applied Anthropology, Indiana University-Purdue University Indianapolis, 2014

BA Anthropology and History, Honors College, Magna Cum Laude, Ball State University, 2012

Academic Honors Diploma Muncie Central High School, 2008

GRANTS AND PUBLICATIONS

2013 J. Wilson (PI), J. Starbuck (Co-PI), B. Brammer (Co-PI), A. Ghoneima (Co-PI).3D Imaging of the Craniofacial Complex Center Collaborative Research Support Grant, Indiana University-Purdue University Indianapolis, "Craniofacial Asymmetry in Mississippian Period Native American Populations," $12000

2012 *The Historical and Cultural Significance of the Irish Folklore Commission*, Published Undergraduate History Department Honors College Thesis, Ball State University

AWARDS AND HONORS

2012 Graduated Magna Cum Laude, Ball State University
2012 History Department Honors College Thesis Award, Ball State University
2012 History Department Outstanding Senior Award, Ball State University
2011 History Department Outstanding Junior Award, Ball State University
2009 Certificate of Special Achievement in Introductory World History, Ball State University
2008-2012 Dean's List Ball State University

FELLOWSHIPS AND SCHOLARSHIPS

2012-2014 IUPUI University Fellowship
2011-2012 Lawrence and Mabel Hurst Scholarship, History Department, Ball State University
2008-2012 Presidential Scholarship, Ball State University
2008 Alumni Association Legacy Scholarship, Ball State University
2008 Hoosier Scholar Award Scholarship

CONFERENCE PARTICIPATION

2012 A Geoarchaeological Investigation of Mounds F and H at Angel Mounds (with senior author A. Williamson and co-authors A. Williamson, K. Williams, and G. Macedaeg). Midwest Archaeological Conference, East Lansing, Michigan. October 18th-20th.

TEACHING EXPERIENCE

2011-2012 Honors Peer Mentor, Ball State University, Muncie, IN

2011-2012 History Department Undergraduate Teaching Fellow, Ball State University, Muncie, IN

RESEARCH EXPERIENCE

2013 Analysis of Mann Site Burned Skeletal Remains

2012 Field Technician, IU/IUPUI Joint Field School in Archaeology at Angel Mound in Evansville, Indiana.

PROFESSIONAL MEMBERSHIPS

Sigma Kappa Sorority Gamma Eta Chapter, Ball State University
Golden Key International Honors Society, Ball State University
Phi Alpha Theta, International Honors History Society, Ball State University
Lambda Alpha National Anthropology Honor Society Alpha Chapter, Ball State University
Phi Kappa Phi National Honor Society, Ball State University

EXTRACURRICULAR UNIVERISTY EXPERIENCE

Anthropology Club, Ball State University
Museum Club, Ball State University
Society for Game Design and Development, Ball State University
University Choral Union, Ball State University